Dynamic Response of the Equivalent Shear Beam (ESB) Container

S.P.G. Madabhushi

CUED/D-SOILS/TR270 (1994)

Synopsis

It is important to simulate the semi-infinite extent of soil in a dynamic centrifuge model test. An Equivalent Shear Beam box was designed and manufactured at the Cambridge University with flexible end walls which simulate the shear deformation of a horizontal soil layer subjected to a model earthquake.

The dynamic response of this ESB box at different 'g' levels is investigated by conducting a centrifuge test. Several earthquakes were fired on the empty ESB box at different 'g' levels. The data from this test are presented in this report. A detailed analysis of the data suggests that the ESB box amplifies a higher frequency component during an earthquake fired at 40g. This higher frequency component increases in strength along the height of the end wall. However the magnitude of this higher frequency component is small when earthquakes are fired at other 'g' levels namely 50g, 60g, 70g and 80g. The higher frequencies of vertical accelerations are amplified at all the 'g' levels at which earthquakes were fired. The amplification of the peak horizontal acceleration increased with the increase of 'g' level. The peak vertical accelerations however were attenuated even ı hough the higher frequency components of the vertical accelerations were amplified.

Contents

DYNAMIC RESPONSE OF THE EQUIVALENT SHEAR BEAM (ESB) CONTAINER

1.0 Introduction

Use of centrifuge modelling in understanding the dynamic behaviour of complex soil-structure systems has established itself as a powerful technique over the past decade. The advances made in the study of earthquake related problems in geotechnical engineering were discussed by Steedman (1991). The principles of dynamic centrifuge modelling are now well understood and the data acquisition techniques and signal processing methods have been standardised. Data from the model tests have been used to validate numerical codes, Madabhushi and Zeng (1993). However there is a need to relate the data obtained from the centrifuge tests to the problems encountered in the field. One of the major concern of a practising engineer about the dynamic centrifuge tests is the boundary conditions created by the model containers. Use of a model container with rigid-smooth end walls will lead to model conditions which are significantly different from the semi-infiite conditions of a soil layer in the field. These differences between a horizontal soil layer in a rigid container and a semi-infiite soil layer in the field arise from the following aspects;

i) strain dissimilarity,
ii) stress dissimilarity and
iii) generation of pressure waves.

The dynamic response of a soil layer can be obtained by treating the soil layer as shear beams. The properties of soil, in general, will vary with the depth of the layer. The dynamic response of such a soil layer will be the same along any vertical plane as shown in Fig. la. However, in a centrifuge model there is no scope for deformation of soil near the rigid end walls as shown in

Fig.lb. This results in a strain dissimilarity between the centrifuge model and the prototype soil layer in the field.

The stress dissimilarity arises from the smoothness of the end walls. The stress state in any soil element in the soil layer is shown in Fig.2. If the end walls were to be smooth the shear stresses are not borne at the boundary resulting in a stress dissimilarity. However, if the end walls were to be rough this dissimilarity will not arise.

Finally the use of rigid wall containers will result in generation of pressure waves from the sides as illustrated in Fig.3. When the rigid container is subjected to base shaking the end walls will cause compression and rarefaction of soil in the vicinity of the boundary. This will result in horizontally travelling pressure waves in the model in addition to the vertically propagating horizontal shear waves from the base. In a prototype soil layer there will be no horizontal pressure waves.

These problems caused by using rigid-smooth end wall containers lead to the concept of using a flexible and frictional end wall containers. An ideal boundary for dynamic centrifuge model tests should satisfy the following criteria;

i) The boundary must have the same dynamic stiffness as the adjacent soil.
ii) It must have the same friction as the adjacent soil.
iii) The model container must have infinite lateral stiffness during the spin-up of the centrifuge so that K_o condition can be maintained.
iv) The frictional end wall must have the same vertical settlement as the soil layer so that there are no initial shear stresses induced at the boundary.

Based on these principles an Equivalent Shear Beam (ESB) model container was developed at the Cambridge University, Zeng (199 1).

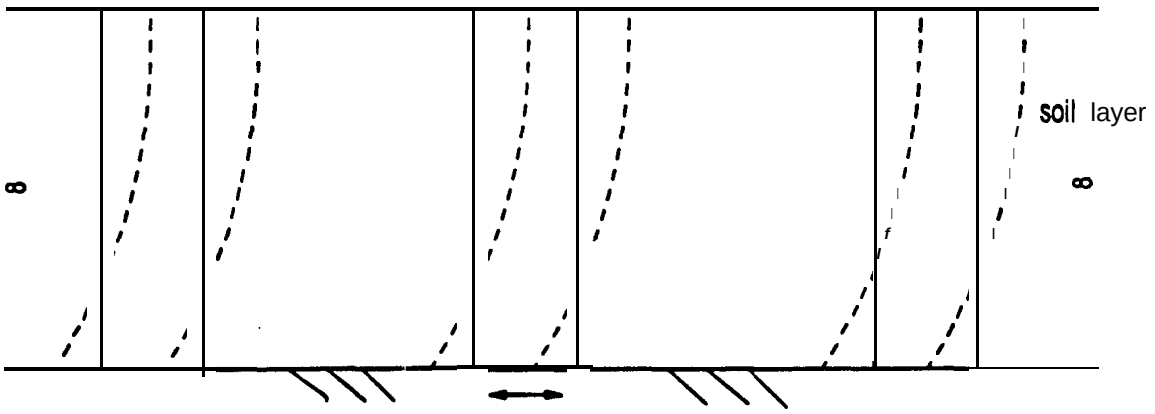

Fig. 1 a Soil deformation in a semi-infinite half space

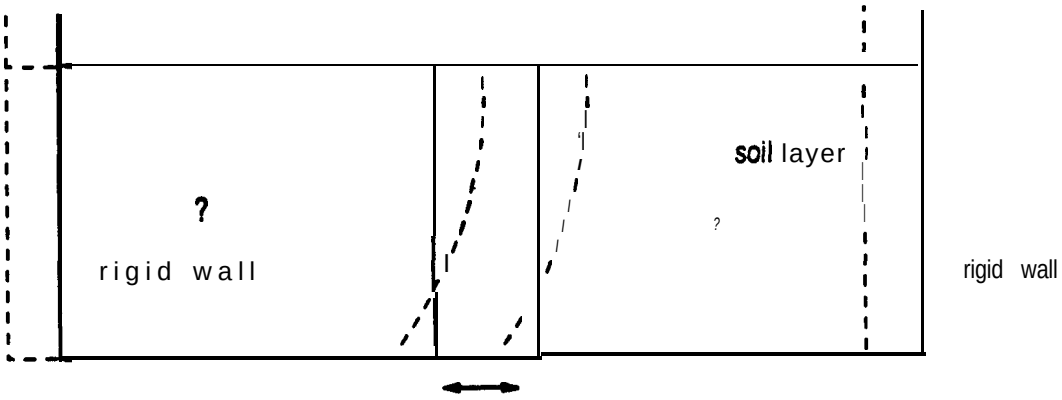

Fig. lb Soil deformation in a centrifuge model with rigid end walls

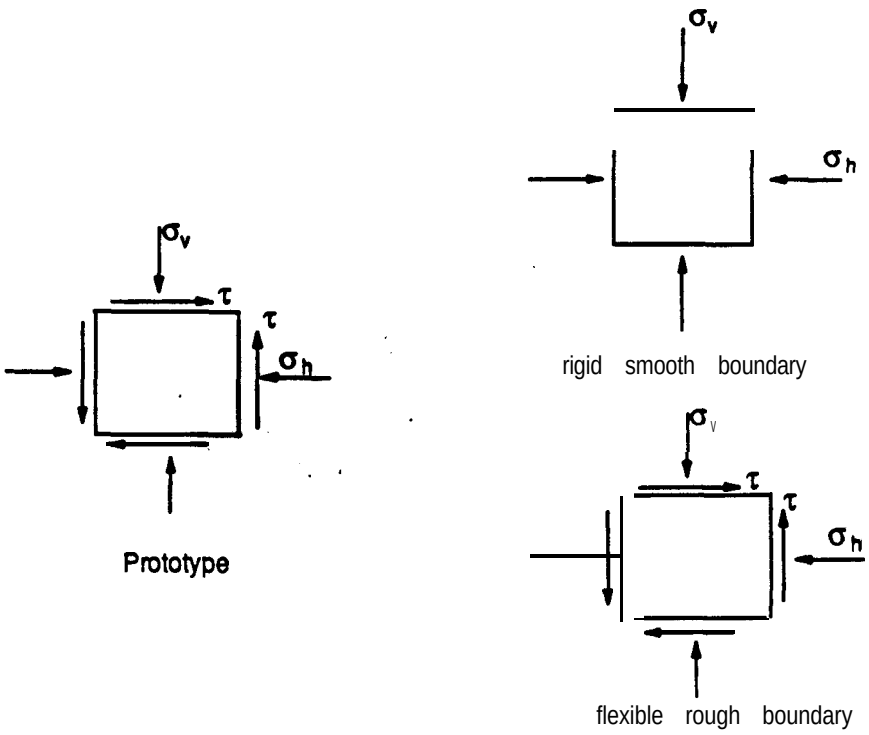

Fig.2 Stress conditions in a soil element in the half space and in the vicinity of the rigid smooth boundary in a centrifuge model

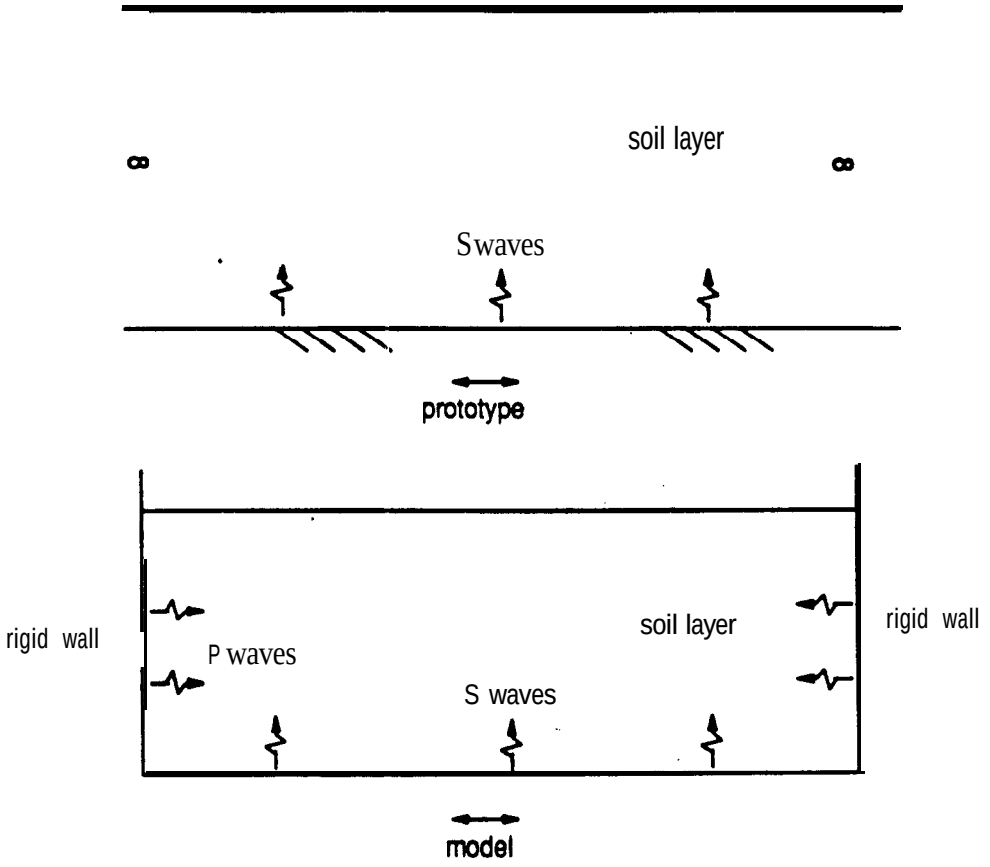

Fig.3 Stress waves in a centrifuge model and in the half space

Design print iples

1) same friction at the boundary
2) same dynamic stiffness
   a) same deflection under seismic loading
   b) same natural frequency

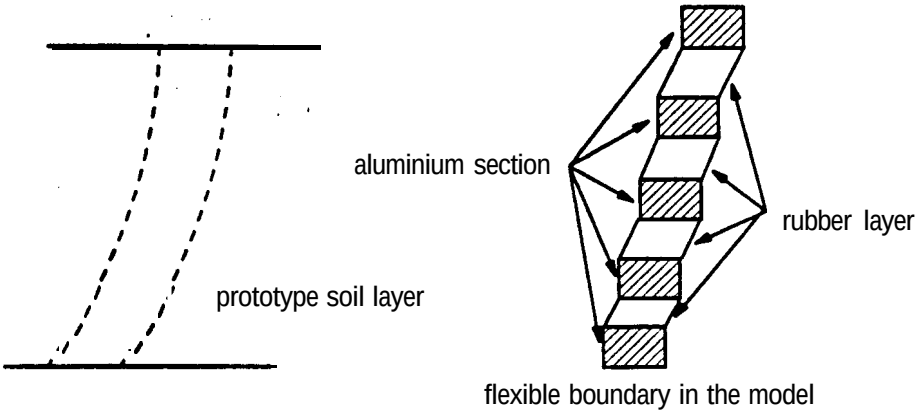

Fig.4 End wall which simulates the soil in the centrifuge model

2.0 Design Principles

The interaction between the end walls of the model container and the soil will be a minimum if the end walls have the same dynamic stiffness and friction as the adjacent soil column during the earthquake loading. This is illustrated in Fig.4. The stiffness of a saturated soil layer however is dependent on the void ratio, the effective confining stress, shear strain amplitude and the magnitude of the excess pore pressures generated during the earthquake loading. It is not possible to have end walls with such variable stiffness. Instead the end walls of the model container can be designed to match the stiffness of a soil layer with specific void ratio subjected to a specific range of shear strains and confining pressures.

Hardin and Dmevich (1972) have suggested a hyperbolic stress-strain relationship for sands given as

$$\tau = G_{max} \frac{\gamma}{1+\frac{\gamma}{\gamma_r}} \quad \ldots\ldots\ldots (1)$$

where G_{max} is the initial tangent modulus, γ_r is the reference shear strain given by

$$\gamma_r = \frac{\tau_{max}}{G_{max}} \quad \ldots\ldots\ldots (2)$$

where τ_{max} is the shear stress at failure. The maximum shear modulus for sands can be obtained from the following empirical formula obtained by Hardin and Dmevich (1972) based on laboratory test data.

$$G_{max} = 100 \frac{[3-e]^2}{[1+e]} \{\sigma_m'\}^{0.5} \quad \ldots\ldots\ldots (3)$$

where 'e' is the void ratio and σ_m' is the mean confining pressure in MPa. The tangent modulus of soil (G_t) may be obtained by using Eq.l as

$$G_t = \frac{d\tau}{d\gamma} = G_{max}\left[1 - \frac{\tau}{\tau_{max}}\right]^2 \quad \ldots\ldots\ldots (4)$$

The stiffness of the soil at different depths is calculated using the above equations and the end wall of the container is designed to have the same overall stiffness by building a section with rigid dural rings and flexible rubber rings placed alternatively. The section is designed such that the end wall will have the same shear deflection as a column of sand. The shear strain induced in such a column of sand may be expressed using Eq. 1 as

$$y = \frac{\tau}{G_{max}} \quad \ldots\ldots\ldots (5)$$

For a particular earthquake the shear stress τ can be calculated as

$$\tau = K_h \gamma_s z \quad \ldots\ldots\ldots (6)$$

where γ is the unit weight of sand, K_h is the peak amplitude of acceleration and z is the depth at which we seek to calculate the shear stress. The maximum shear stress depends on the initial K_o state of the soil and the shear stress due to the earthquake and can be obtained from the Mohr's circles for initial and fmal stress states shown in Fig.5 From this figure we can derive the following relation for maximum shear stress.

$$\tau_{max} = \sqrt{\{0.5(1+K_o)\sigma_v' \sin\varphi\}^2 - \{0.5(1-K_o)\sigma_v'\}^2} \quad \ldots\ldots (7)$$

where φ is the internal friction angle and the σ_v' is the effective stress. Knowing τ_{max} the reference strain γ_r is calculated using Eq.2. Thus the shear strain γ at any depth can be calculated in a similar fashion. Now the total shear displacement relative to the base can be obtained as

$$\delta(z) = \int_H^z -\gamma(z)dz = \int_H^z -\frac{\tau}{G_{max} - \frac{\tau}{\gamma_r}}dz \quad \ldots\ldots\ldots (8)$$

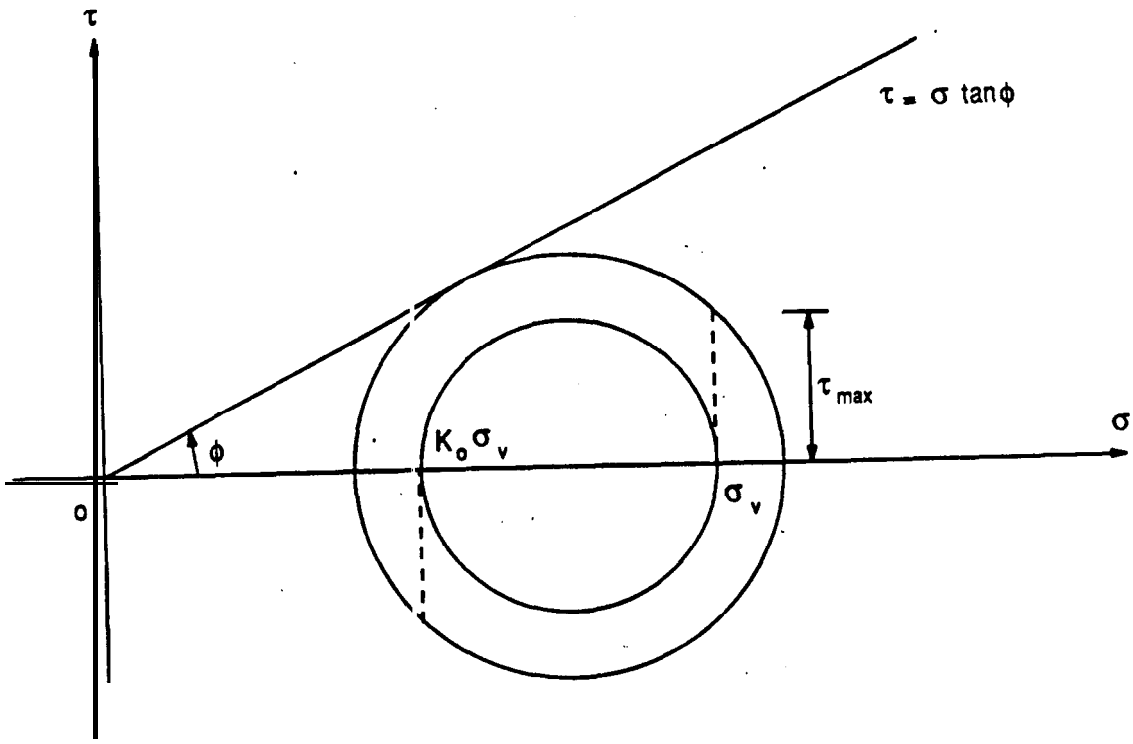

Fig.5 Mohr circle for K_o state and for failure state

The Cambridge Equivalent Shear Beam (ESB) box was designed for a thickness of soil layer of 10m with a void ratio of 0.75 and a dry density of 15 kN/m^3 and a peak acceleration of 30%. The three dimensional view of the ESB box is presented in Fig.6. The shear displacement of the end walls of the ESB box under design conditions listed above is shown in Fig.7. This shear displacement must match the shear displacement of the soil as shown in Fig.8. Performance of the ESB box was confirmed by using the data from a centrifuge test in which the horizontal soil layer was tested under design conditions, Schofield and Zeng (1992). In Fig.9 the observed shear displacement and the calculated (design) shear displacements are shown.

3.0 Use of Equivalent Shear Beam (ESB) box in centrifuge tests

Several centrifuge tests were carried out using the equivalent shear beam box as the model container, Zeng (1992), Madabhushi (1993). The ESB box was designed for specific 'g' level, soil density, void ratio and earthquake strength as explained in earlier section. In some of the tests cited above not all of these conditions could be satisfied. It is important to determine the dynamic response of the Equivalent Shear Beam box in order to delineate the effects of the boundary on the soil model during earthquake loading. This is particularly important when the ESB box is used at different 'g' levels and with soil properties and earthquake magnitudes which are different from the design values.

The natural frequency of the end walls of the ESB container may be determined by using the Rayliegh's method which involves equating the peak kinetic energy to the peak potential energy of the system. Assuming a deflected shape of the end wall as

$$\delta(z,t) = \delta(z)\sin\varpi_n t \quad \ldots\ldots\ldots (9)$$

where ϖ_n is the natural frequency. Differentiating Eq.9 we obtain the velocity function as

$$v(z,t) = \varpi_n \delta(z)\cos\varpi_n t \quad \ldots\ldots\ldots (10)$$

giving the maximum kinetic energy of

$$(KE)_{max} = \int_0^H 0.5\frac{\gamma_s}{g}\delta(z)\varpi_n^2 dz \quad \ldots\ldots*\ldots\ldots (11)$$

The maximum potential energy is

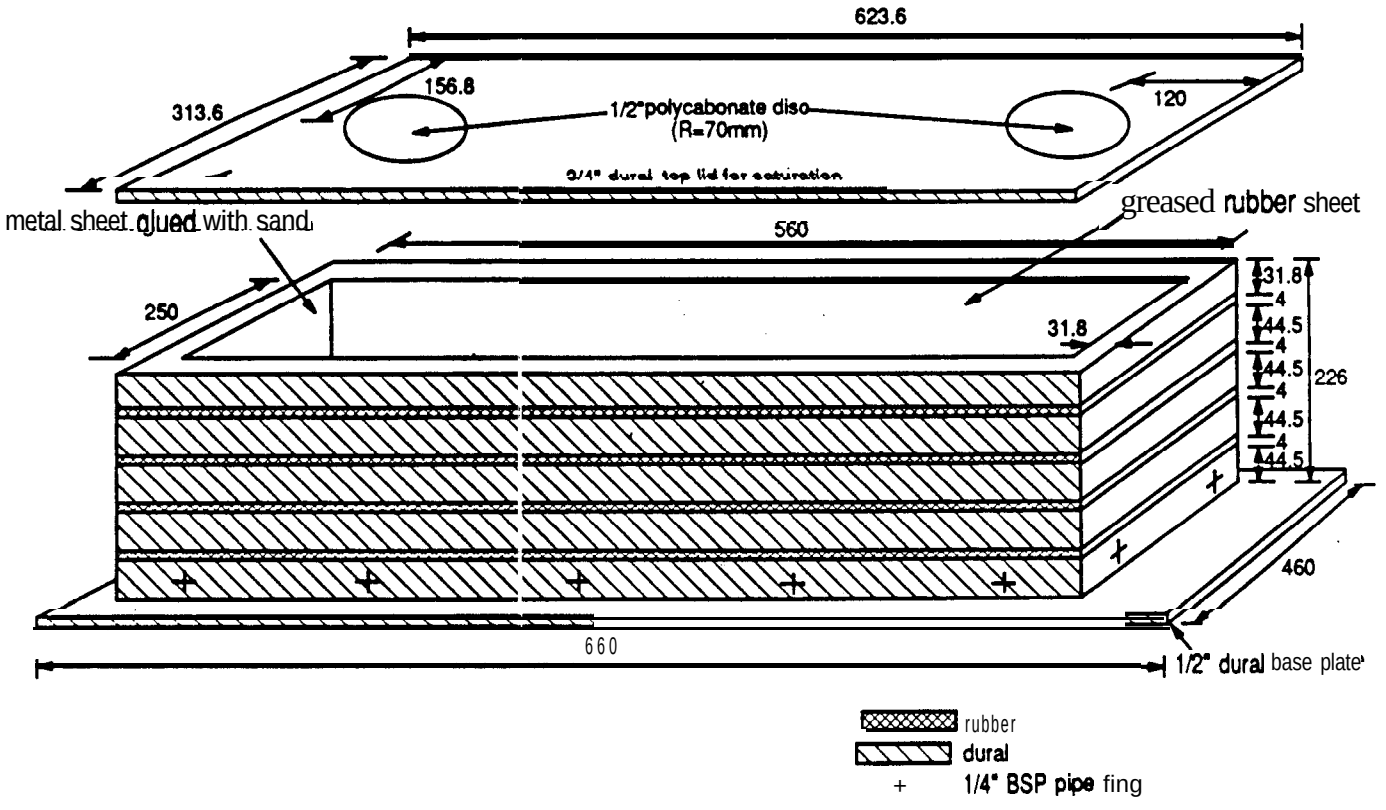

Fig.6 A three dimensional view of the Cambridge Equivalent Shear Beam (ESB) container

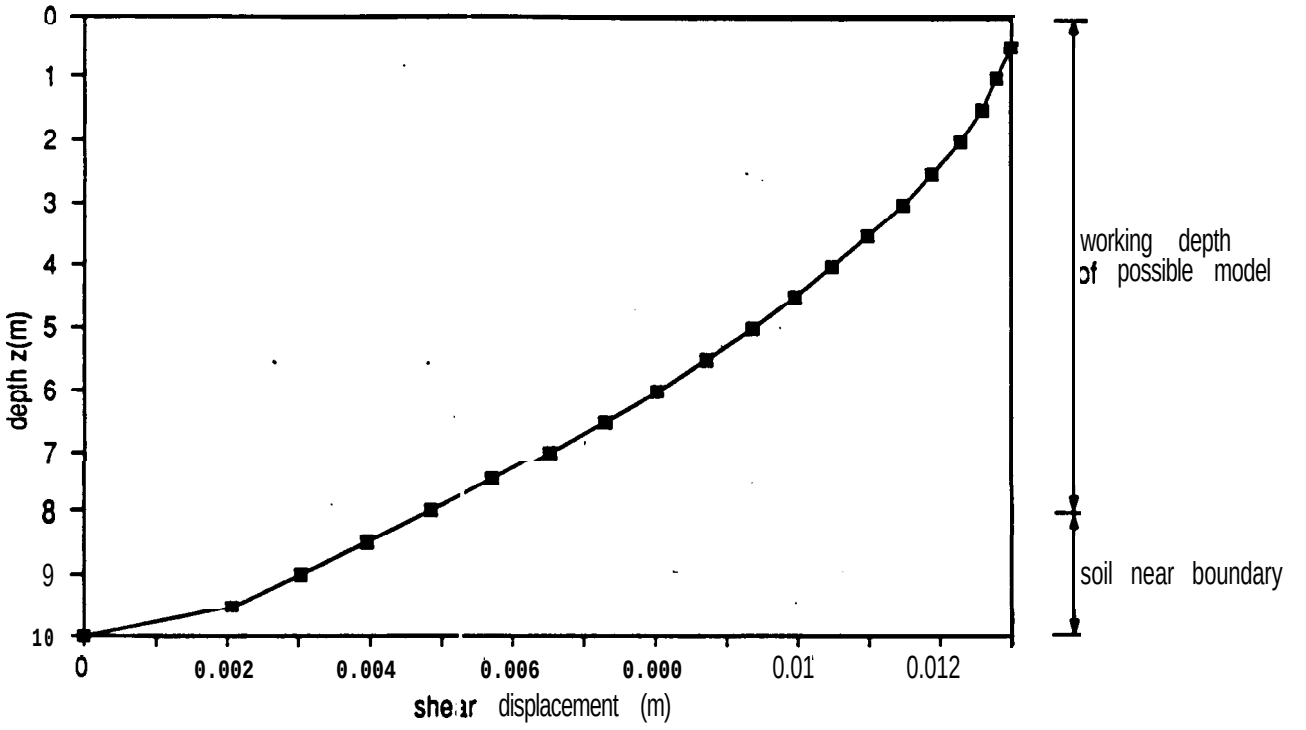

Fig.7 Calculated soil deformation with depth

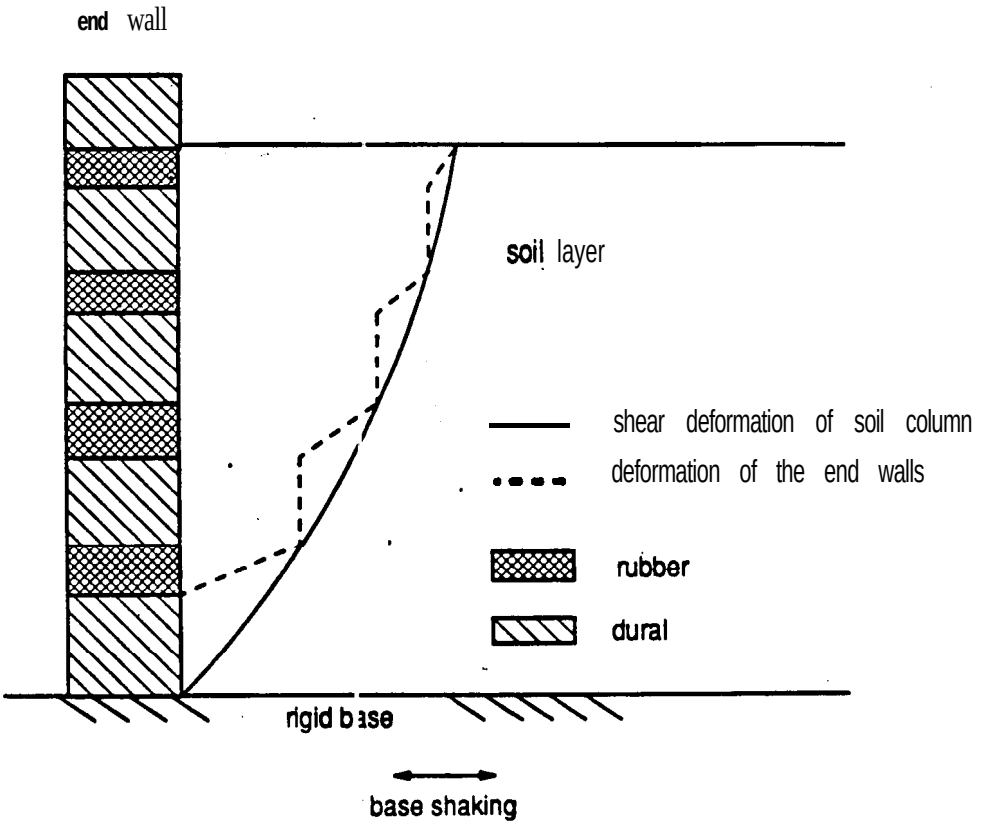

Fig.8 Deformation of end walls and the soil deformation

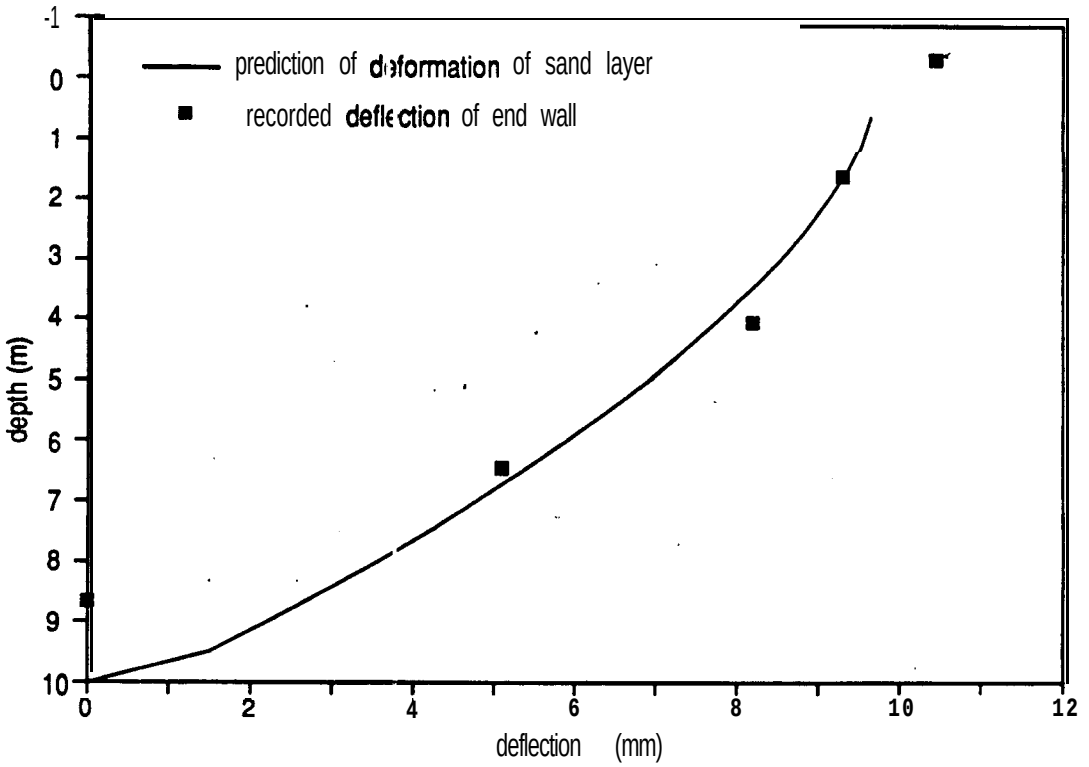

Fig.9 Observed and estimated shear deformation of the end walls

$$(PE)_{max} = \int_0^H 0.5(\tau_{max}\gamma_{max})dz \ldots\ldots\ldots\ldots (12)$$

Equating 11 and 12 the natural frequency ϖ_n of the end wall is obtained. For the design values of the ESB box the natural frequency of the wall was computed to be 130 Hz.

4.0 Dynamic response of the ESB box

In this report the data from a series of earthquakes fired on the Equivalent Shear Beam box at different 'g' levels will be presented. In this centrifuge test, designated as MG- 1, the empty ESB box was subjected to earthquakes so that the dynamic response of the ESB box can be identified. The ESB box was instrumented using accelerometers and LVDT's. The dynamic response of the ESB box at each 'g' level will be established using the data from the centrifuge test.

A total of five earthquakes were fired during this centrifuge test and are designated as EQ-1 to EQ-5. In Table 1 each of the earthquake, its strength and the 'g' level at which it was fired are presented.

Table 1 Strength of earthquakes

EQ Number	G Level	Peak acceleration (% g)
1	40 g	14.8
2	50 g	25.5
3	70 g	19.3
4	80 g	25.6
5	60 g	14.0

5.0 Instrumentation

5. I Accelerometers

In the centrifuge tests reported here miniature piezoelectric accelerometers manufactured by D.J. Birchall were used to measure acceleration in the soil, on the model container and on the block building models during earthquakes. The device has a resonant frequency of about 50 kHz and a maximum error of 5%. The weight of the transducer is about 5 grams. Fig.10 shows the dimensions of the transducer.

5.2 Displacement measuring device

The displacement of the model container and the block building models during centrifuge tests was measured by linear variable differential transformers (LVDTs) manufactured by Sangamo. The dimensions of the transducer is shown in Fig. 11. Each transducer weighs about 36 grams. The short body has a sensitive range of 10 VDC. Since the transducer has a comer frequency of 57.7. Hz, the response of this type of LVDT to high frequency signals is limited by the inertia characteristics of the devices. In the model earthquakes the magnitude and phase of high frequency cyclic displacements recorded by a LVDT of this type does not correspond to the magnitude and phase of the actual cyclic displacement. However the lower frequency components of displacements are correctly recorded so that the record of a LVDT transducer during a model earthquake shows the mean displacements reasonably well and the difference between readings before and after a model earthquake correctly reflects the overall displacements as a result of an earthquake.

6.0 Positioning of the instruments

The positioning of the accelerometers and the LVDT's is shown in Fig.12. The accelerometers were placed at different heights on either side to measure the horizontal accelerations. Vertical accelerations were measured at the base and also at the top of the end walls to identify any rocking of the box. ACC's 3441 and 1225 were placed at the same height but on either side of

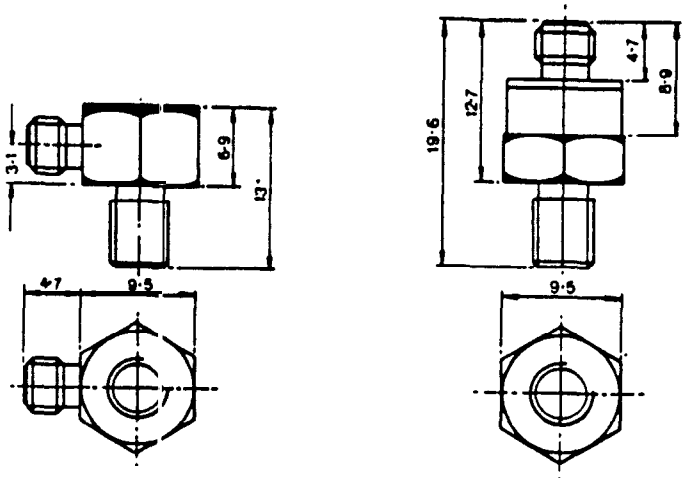

unit: mm mass: 0.005 kg

Fig. 10 Dimensions of a miniature accelerometer

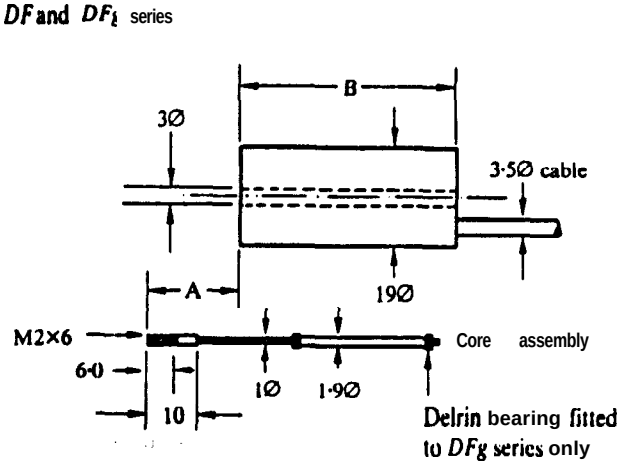

unit: mm mass: 0.036 kg

Fig. 11 Dimensions of a small stroke LVDT

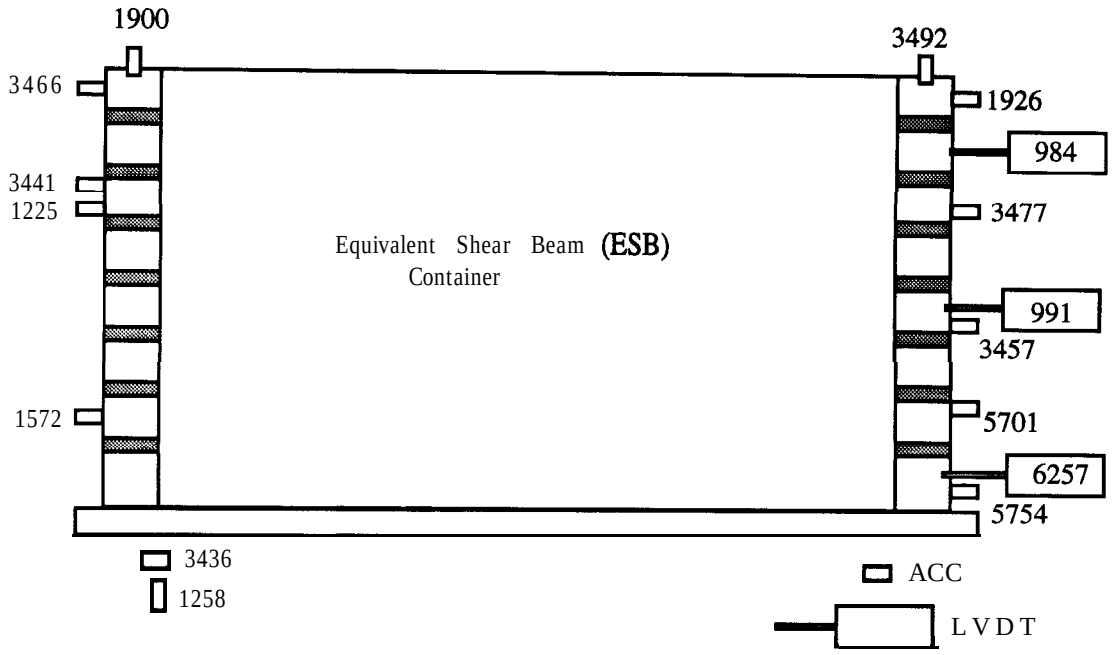

Fig. 12 Placement of instruments in centrifuge test MG- 1

Location of the Instruments

Accelerometer	x (mm)	y(mm)	z(mm)
1926	**-33**	**115**	205
3477	-33	115	160
3457	-33	115	115
5701	-33	115	70
5754	-33	115	25
3466	625	115	208
3441	625	115	160
1225	625	-115	160
1572	625	115	120
3492 (v)	-20	40	225
1900 (v)	610	40	225

the longitudinal axis of the ESB box so that they will detect any twisting of the ESB box during earthquake loading.

7.0 Data from the Centrifuge tests

All the data presented in this section were subject to a low pass digital filter to remove the high frequency components superposed on the signals due to the electrical noise in the slip rings of the centrifuge. The cut off frequency of the filter was 2000.0 Hz. The filter characteristics are presented in Fig. 13.

The data from the centrifuge tests are presented in Figs.14 to 28. In these figures the magnitude of acceleration is expressed as a percentage of the centrifugal acceleration at which the model is being tested. The magnitude of displacement is in 'mm'. The analysis of the data is presented in the next section.

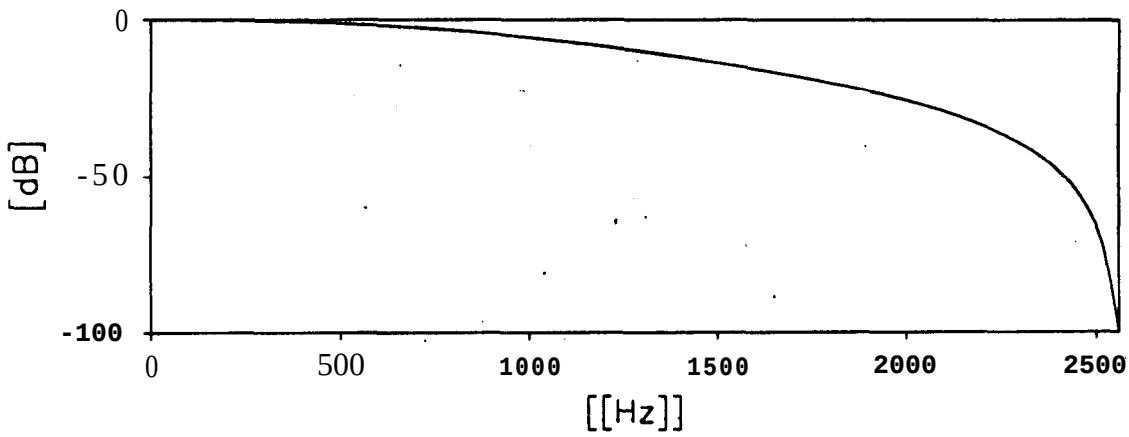

Fig. 13 Filter characteristics

1280 data points plotted per complete transducer record

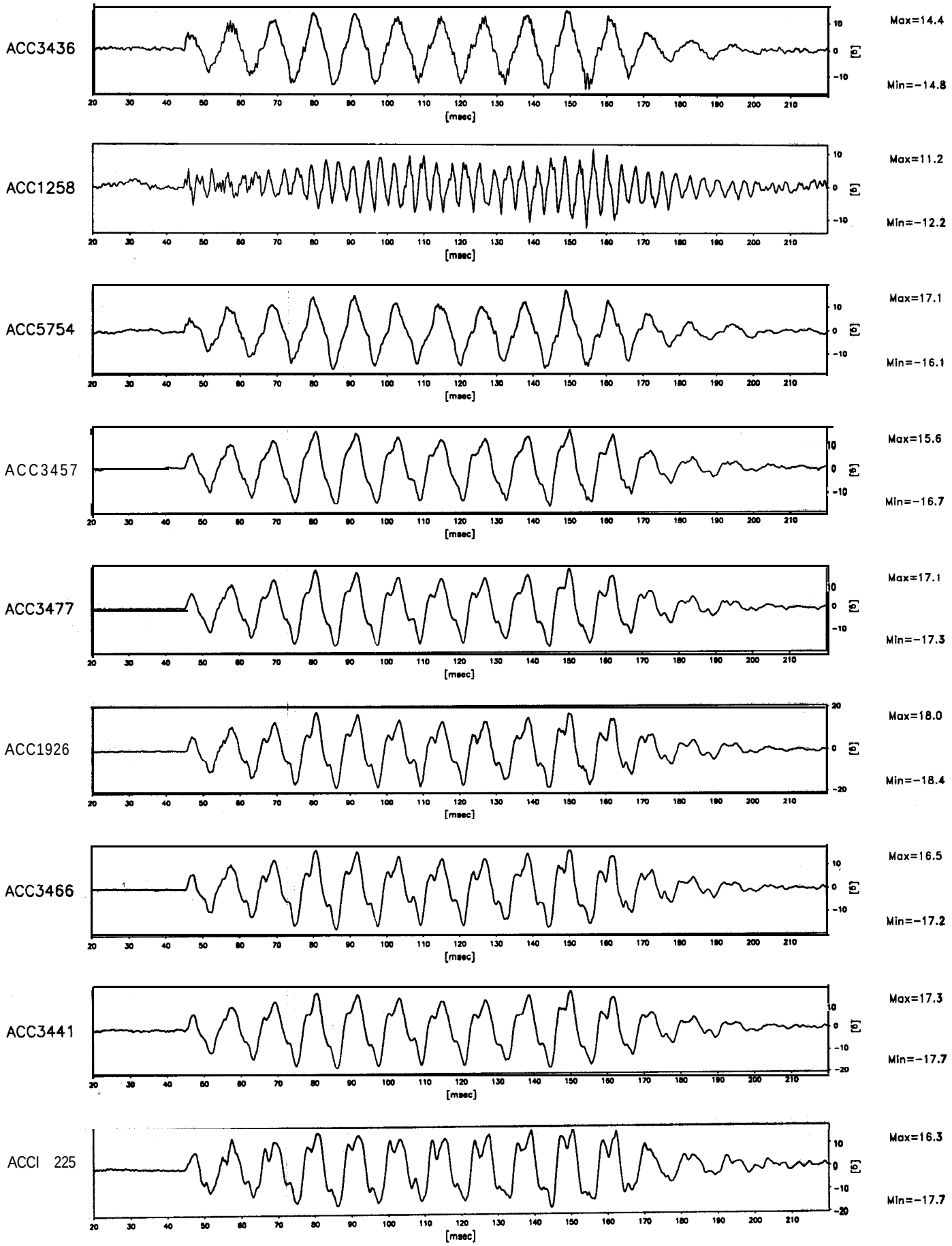

Scales : Model

TEST MG-1 MODEL DRY FLIGHT - 1	EQ-1	SHORT TERM TIME RECORDS	G Level 40	FIG.NO. 14

676 data points plotted per complete transducer record

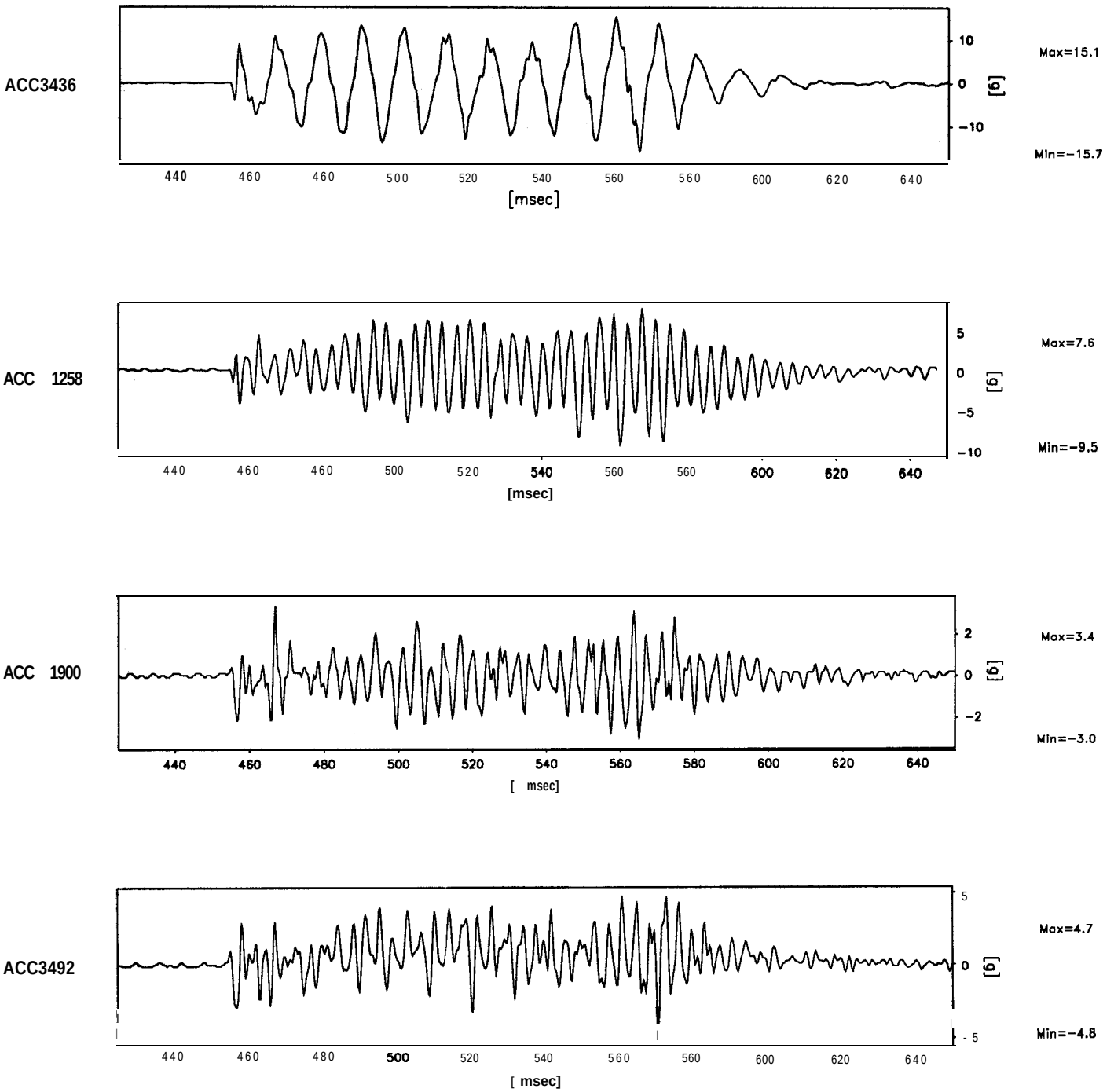

Scales : Model

TEST MG-1 MODEL DRY FLIGHT – 1	EQ–1	SHORT TERM TIME RECORDS	G Level 40	FIG.NO. 15

1280 data points plotted per complete transducer record

ACC3436

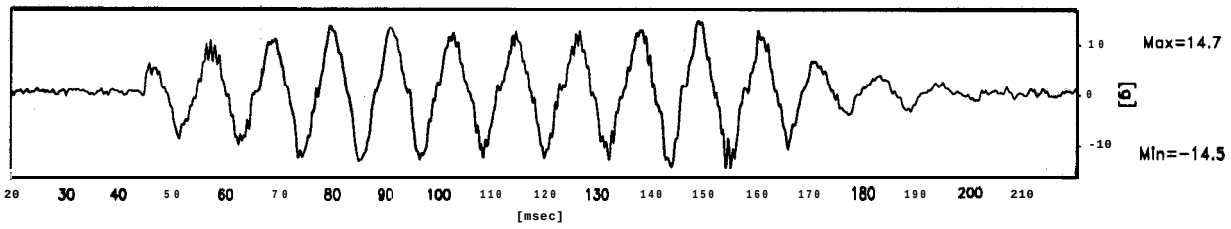

ACC 1572

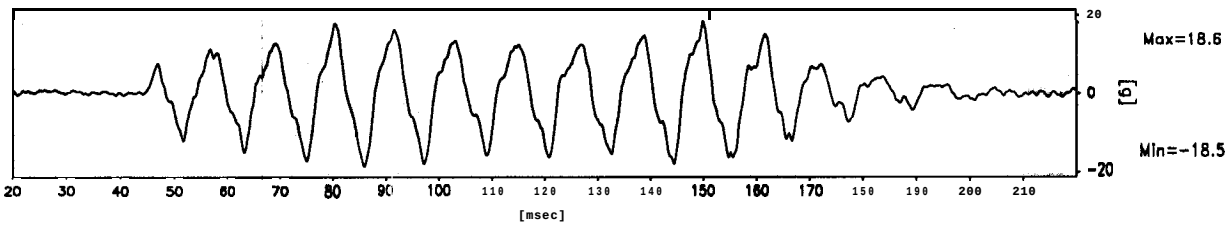

ACC5701

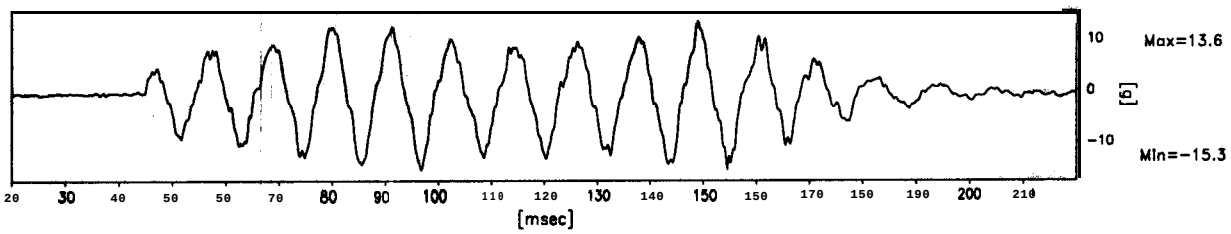

LVDT984

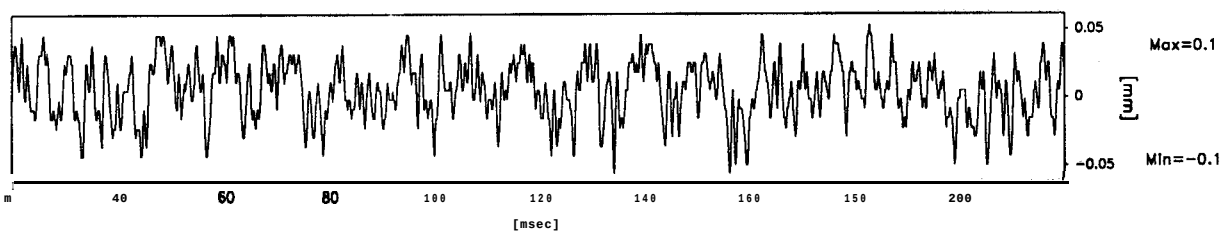

LVDT991

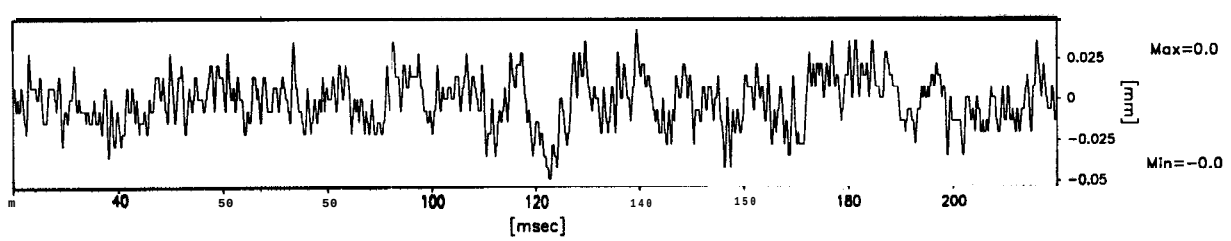

LVDT6257

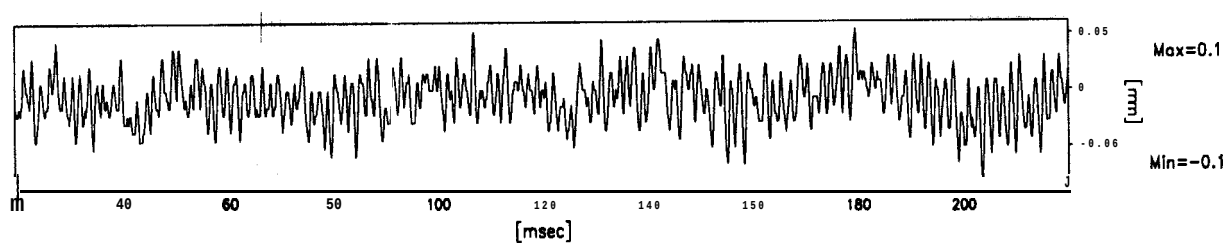

Scales : Model

TEST MG-1 MODEL DRY FLIGHT -1	EQ-1	SHORT TERM TIME RECORDS	G Level 40	FIG.NO. 16

1280 data points plotted per complete transducer record

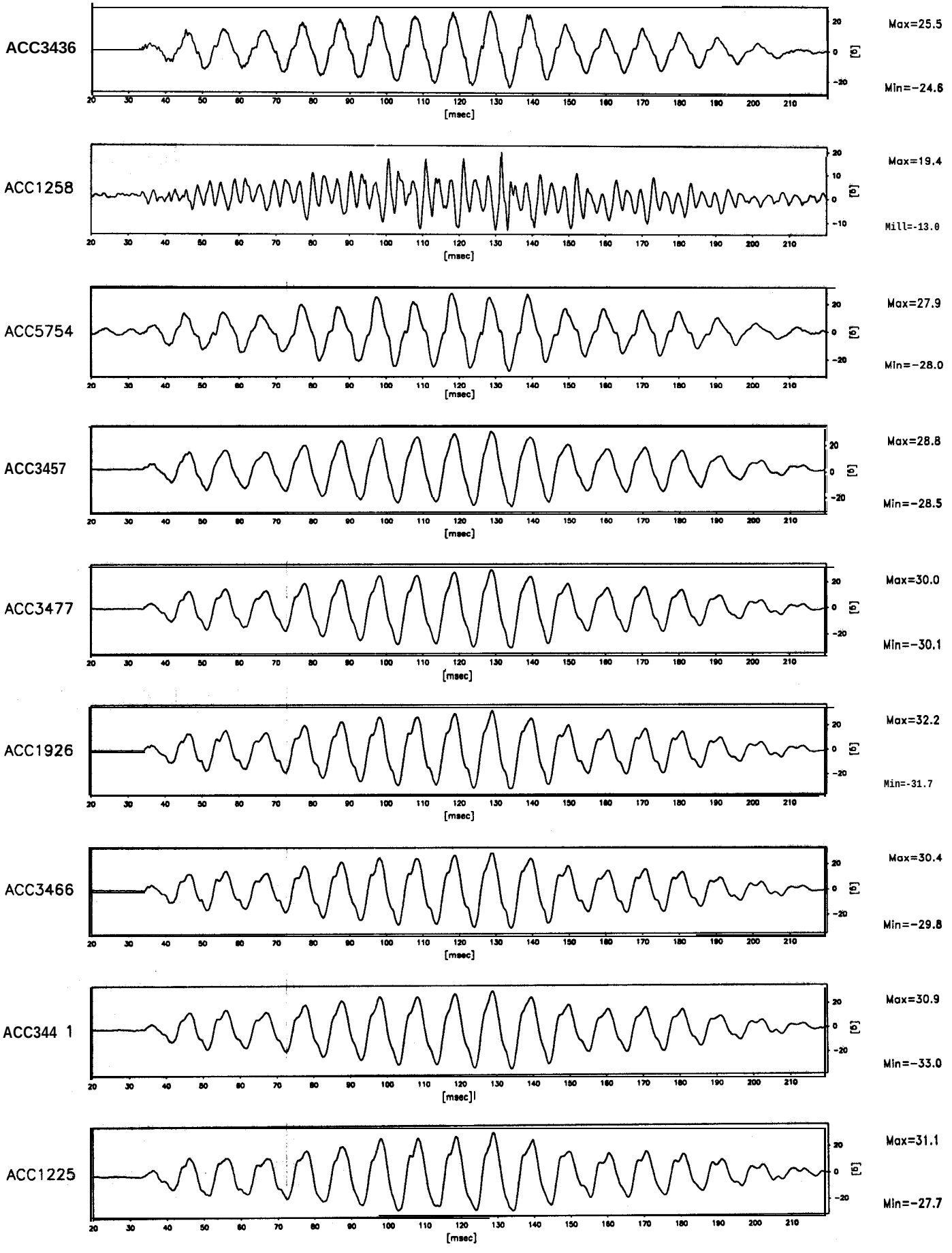

Scales : Model

TEST MG-1 MODEL DRY FLIGHT - 1	EQ-2	SHORT TERM TIME RECORDS	G Level 50	FIG.NO. 17

677 data points plotted per complete transducer record

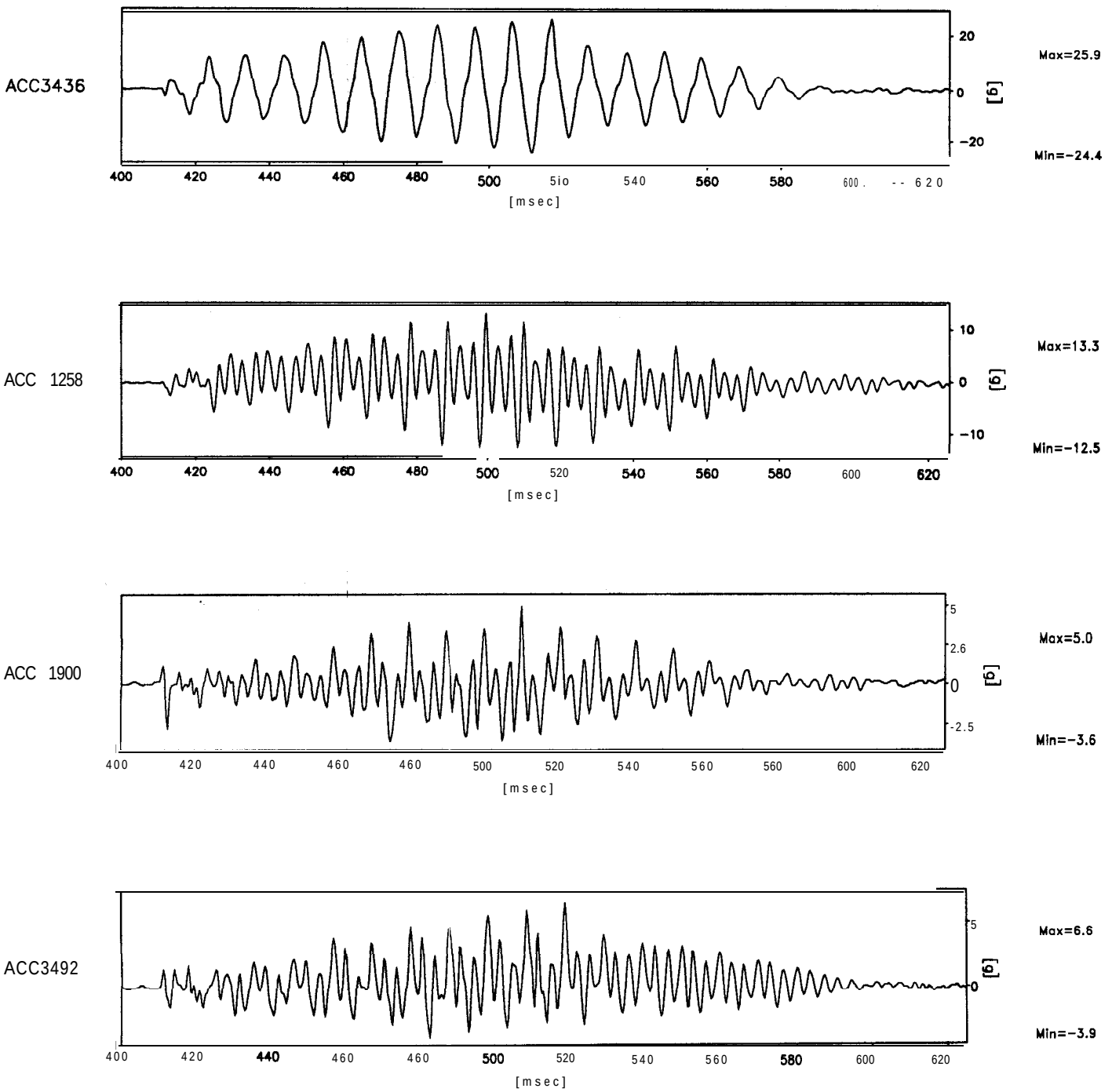

Scales : Model

TEST MG-1 MODEL DRY FLIGHT -1	EQ-2'	SHORT TERM TIME RECORDS	G Level 50	FIG.NO. 18

1280 data points plotted per complete transducer record

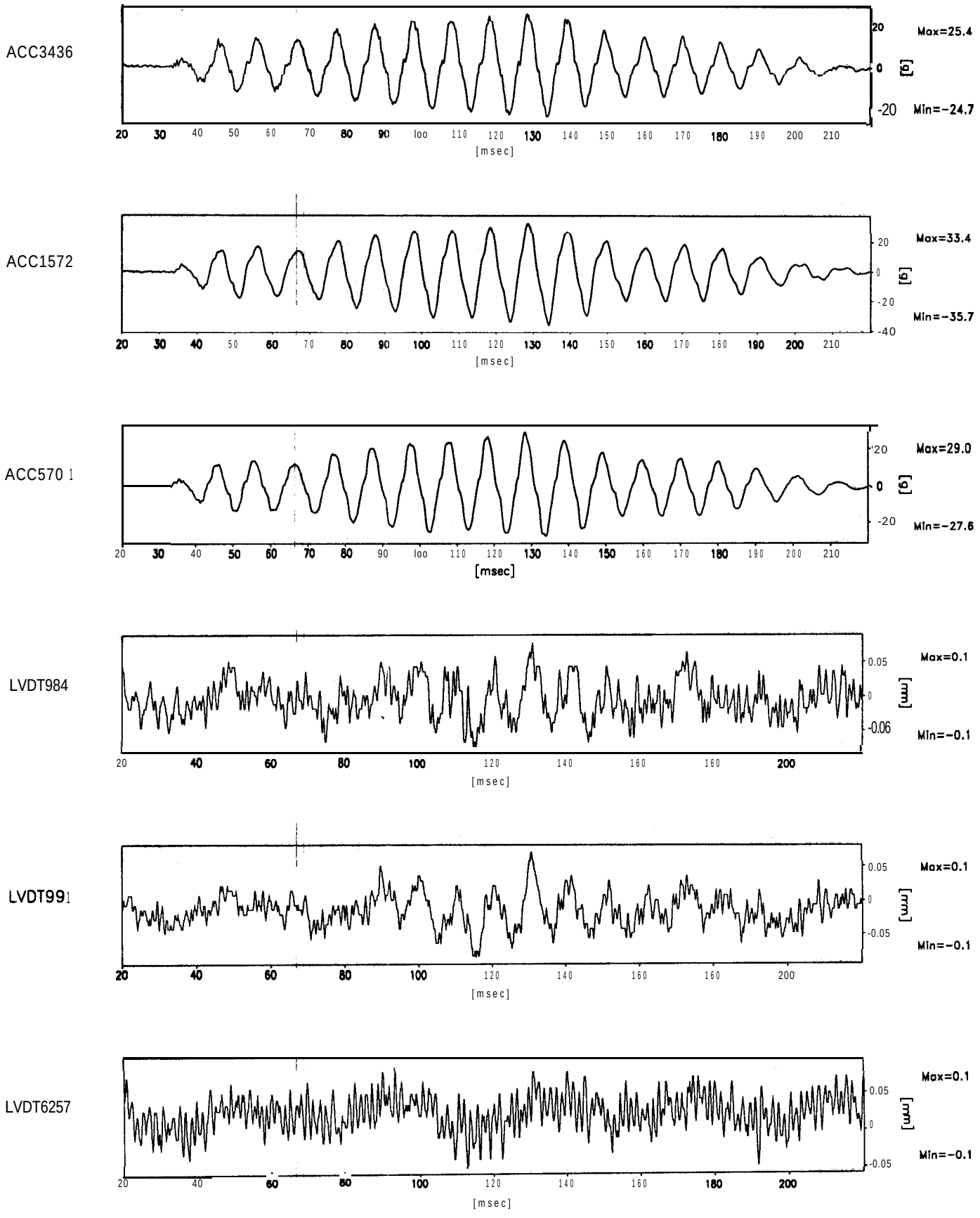

Scales : Model

TEST MG-1 MODEL DRY FLIGHT -1	EQ-2	SHORT TERM TIME RECORDS	G Level 50	FIG.NO. 19

959 data points plotted per complete transducer record

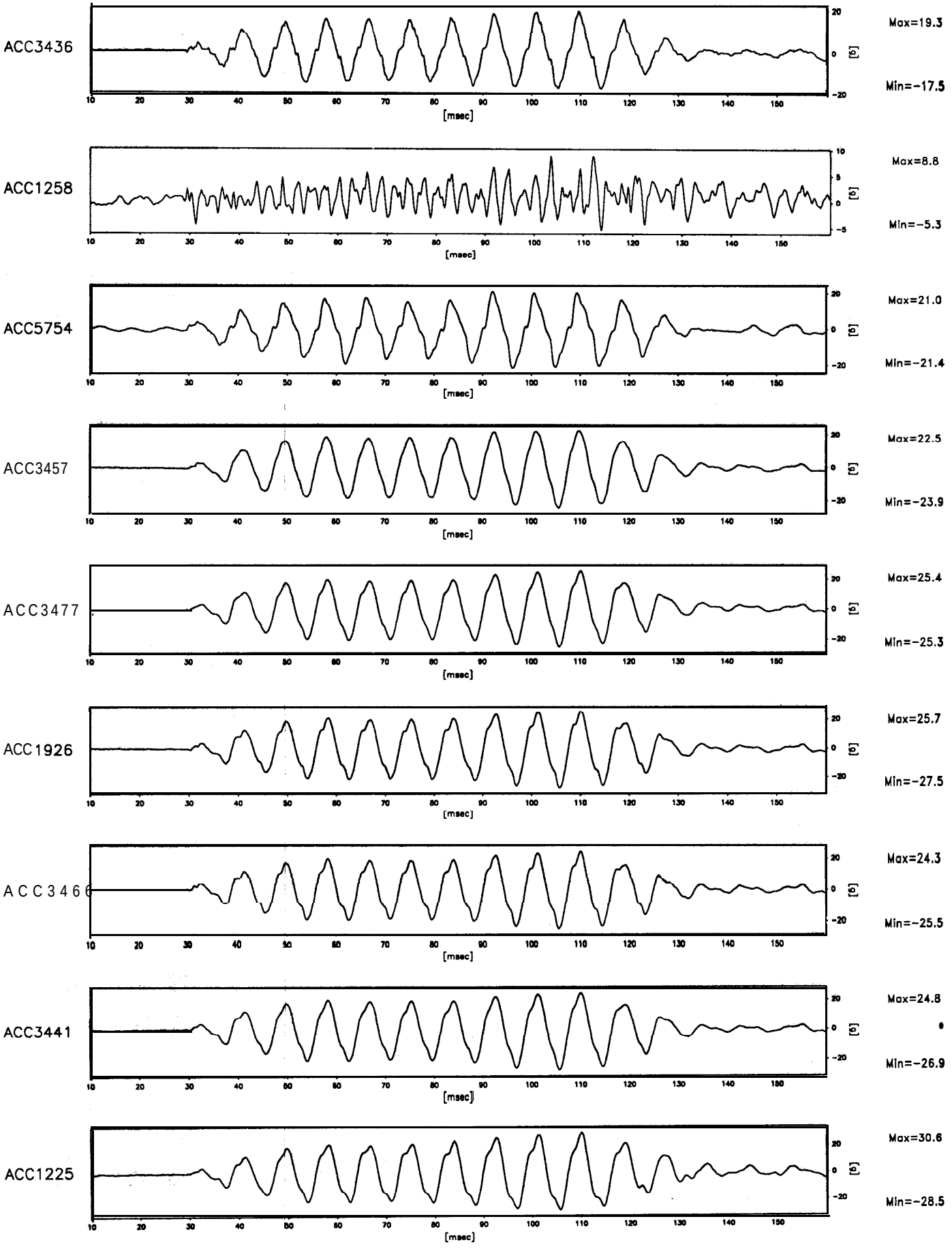

Scales : Model

TEST MG-1 MODEL DRY FLIGHT -1	EQ-3	SHORT TERM TIME RECORDS	G Level 70	FIG.NO. 20

601 data points plotted per complete transducer record

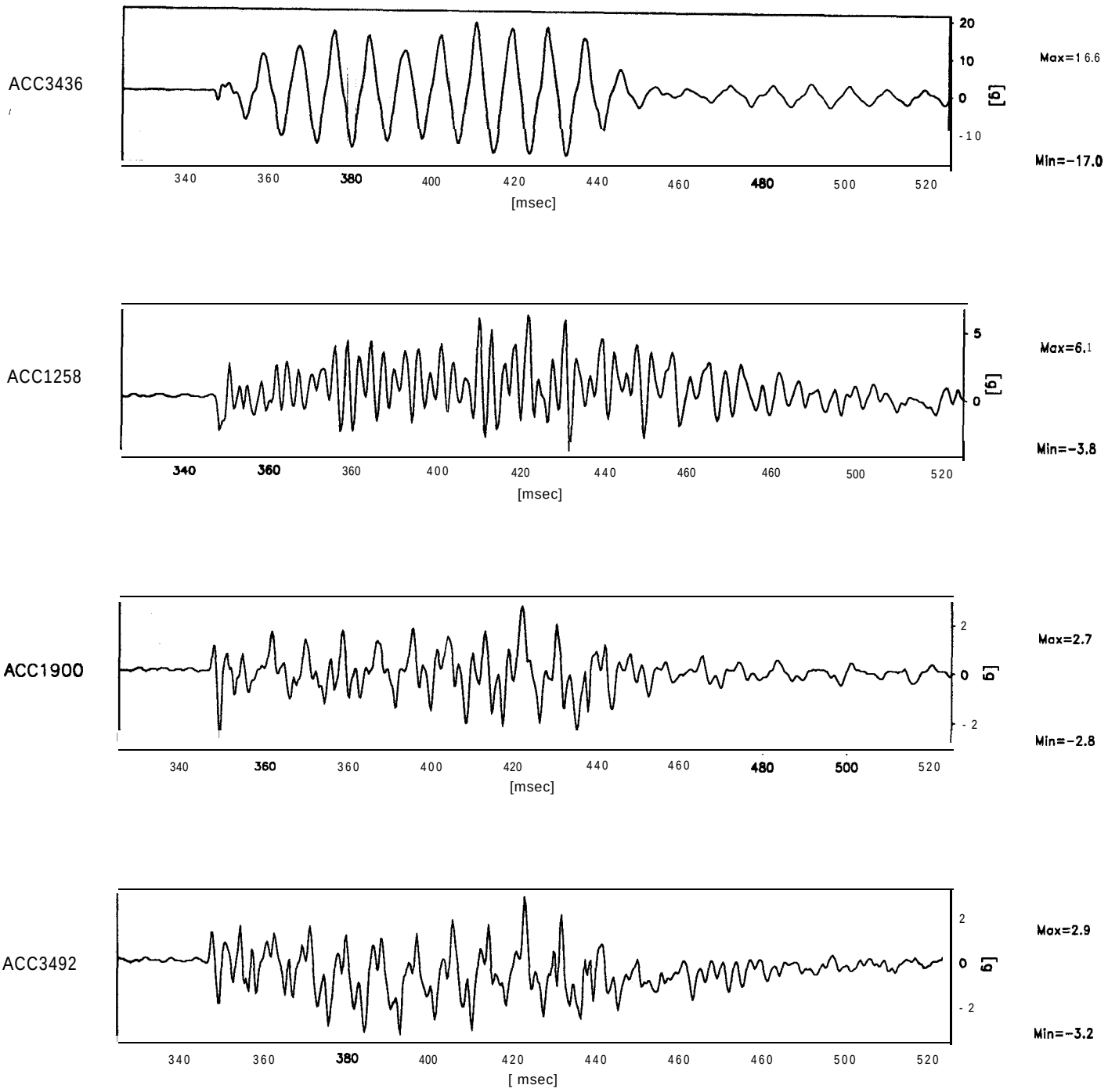

Scales : Model

TEST MG-1 MODEL DRY FLIGHT – 1	EQ-3	SHORT TERM TIME RECORDS	G Level 70	FIG.NO. 21

959 data points plotted per complete transducer record

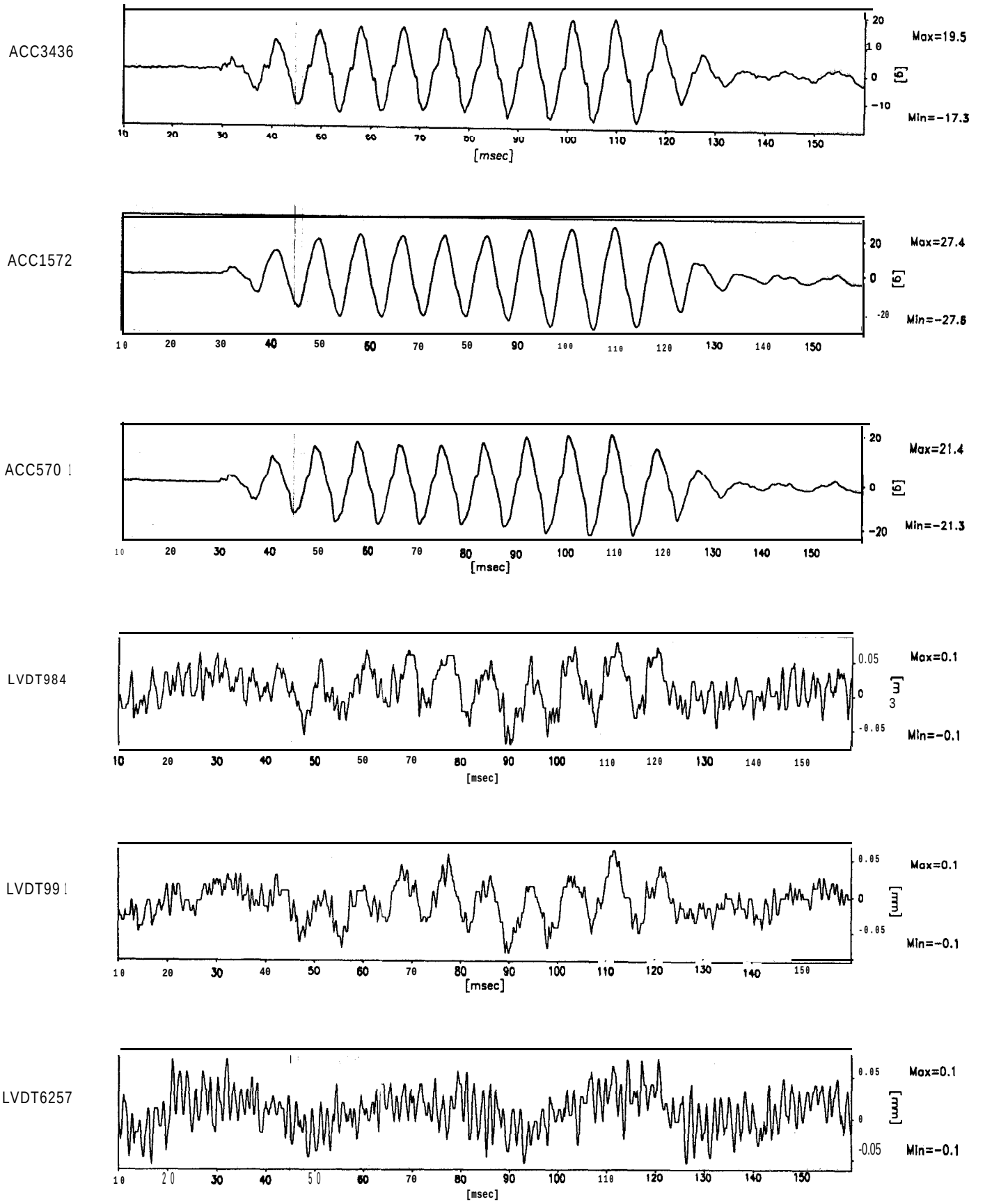

Scales : Model

TEST MG-1 MODEL DRY FLIGHT –1	EQ–3	SHORT TERM TIME RECORDS	G Level 70	FIG.NO. **22**

959 data points plotted per complete transducer record

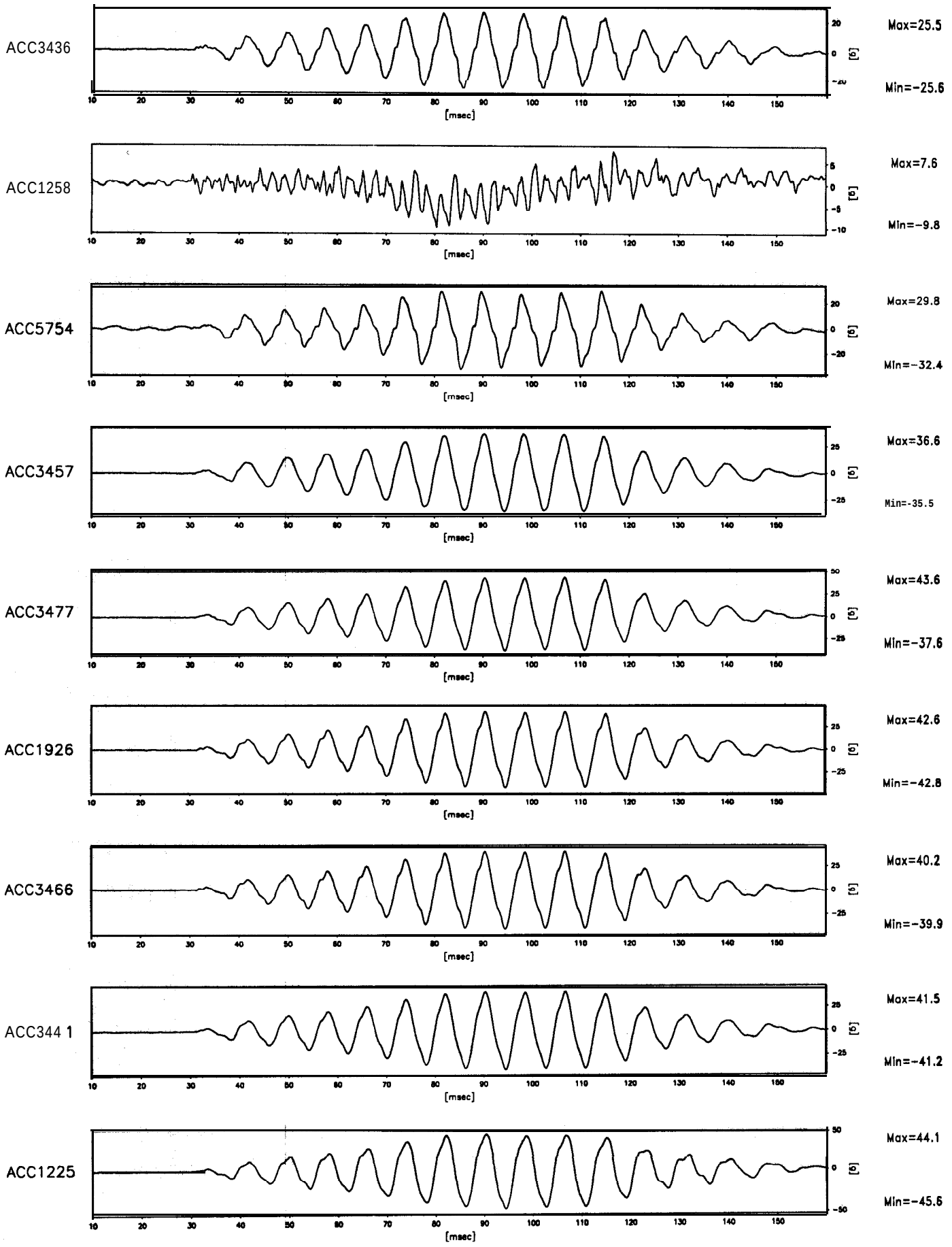

Scales : Model

TEST MG-1 MODEL DRY FLIGHT -1	EQ-4	SHORT TERM TIME RECORDS	G Level 80	FIG.NO. 23

601 data points plotted per complete transducer record

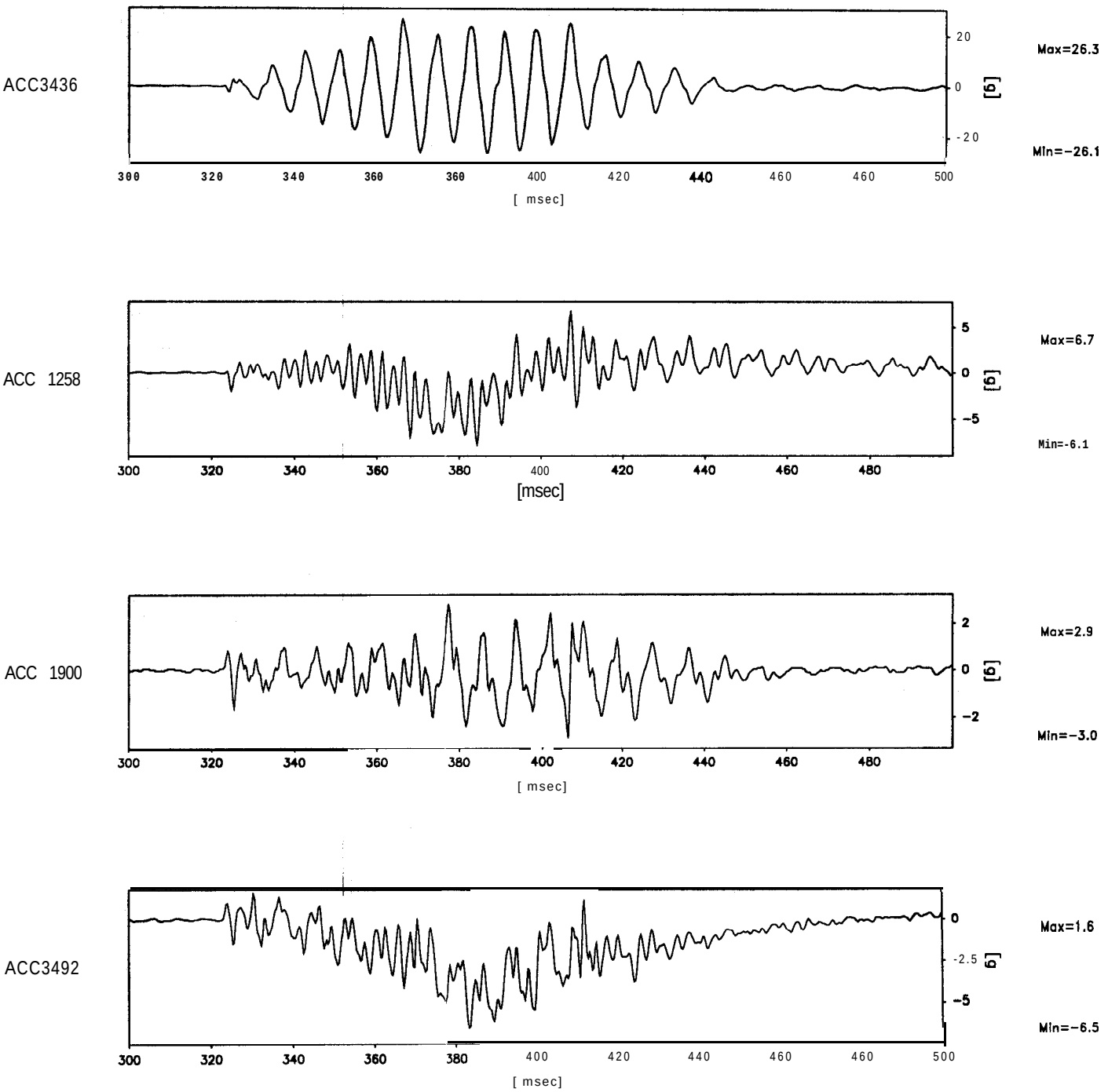

Scales : Model

TEST MG-1 MODEL DRY FLIGHT -1	EQ-4'	SHORT TERM TIME RECORDS	G Level 80	FIG.NO. 24

959 data points plotted per complete transducer record

ACC3436

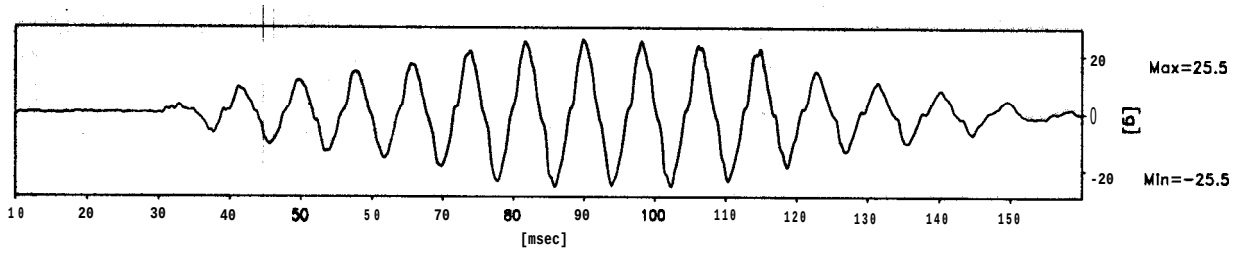

ACC1572

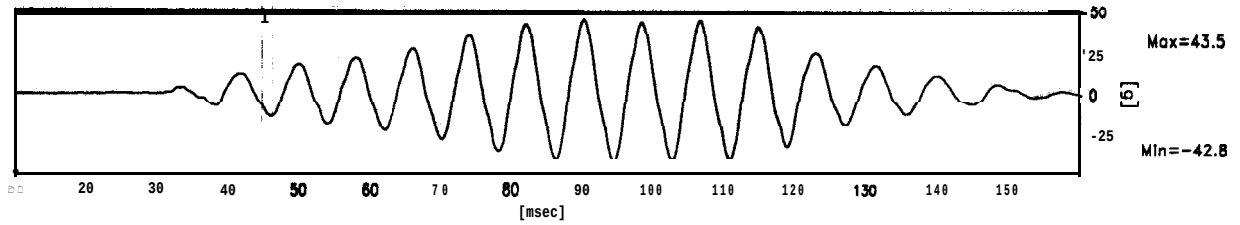

ACC5701

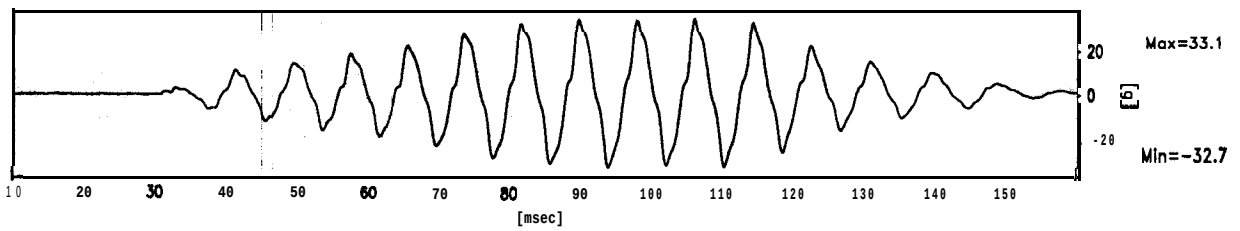

LVDT984

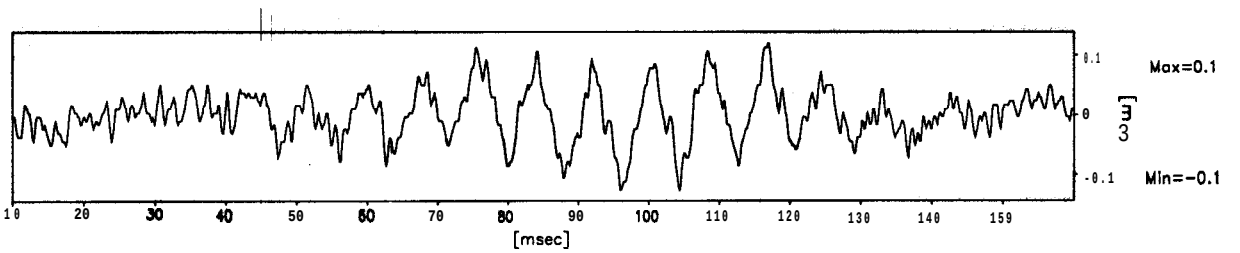

LVDT991

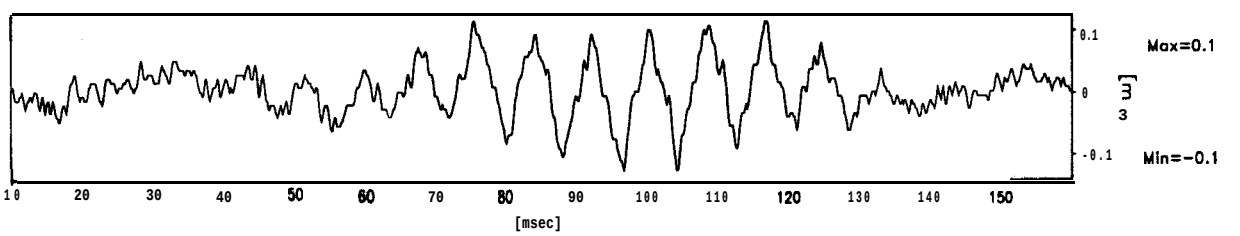

LVDT6257

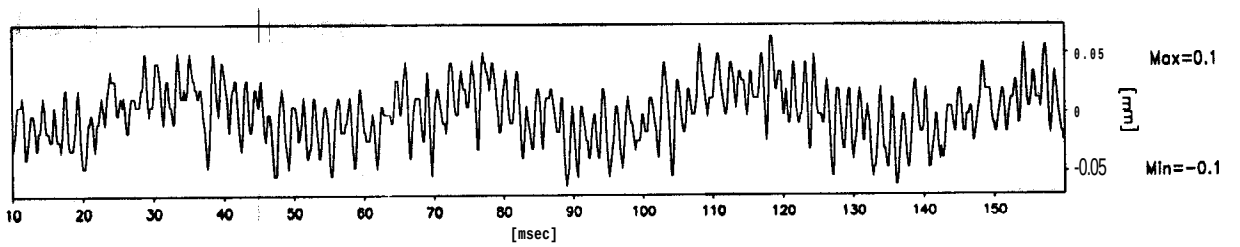

Scales : Model

TEST MG-1 MODEL DRY FLIGHT -1	EQ-4	SHORT TERM TIME RECORDS	G Level 80	FIG.NO. 25

1152 data paints platted per complete transducer record

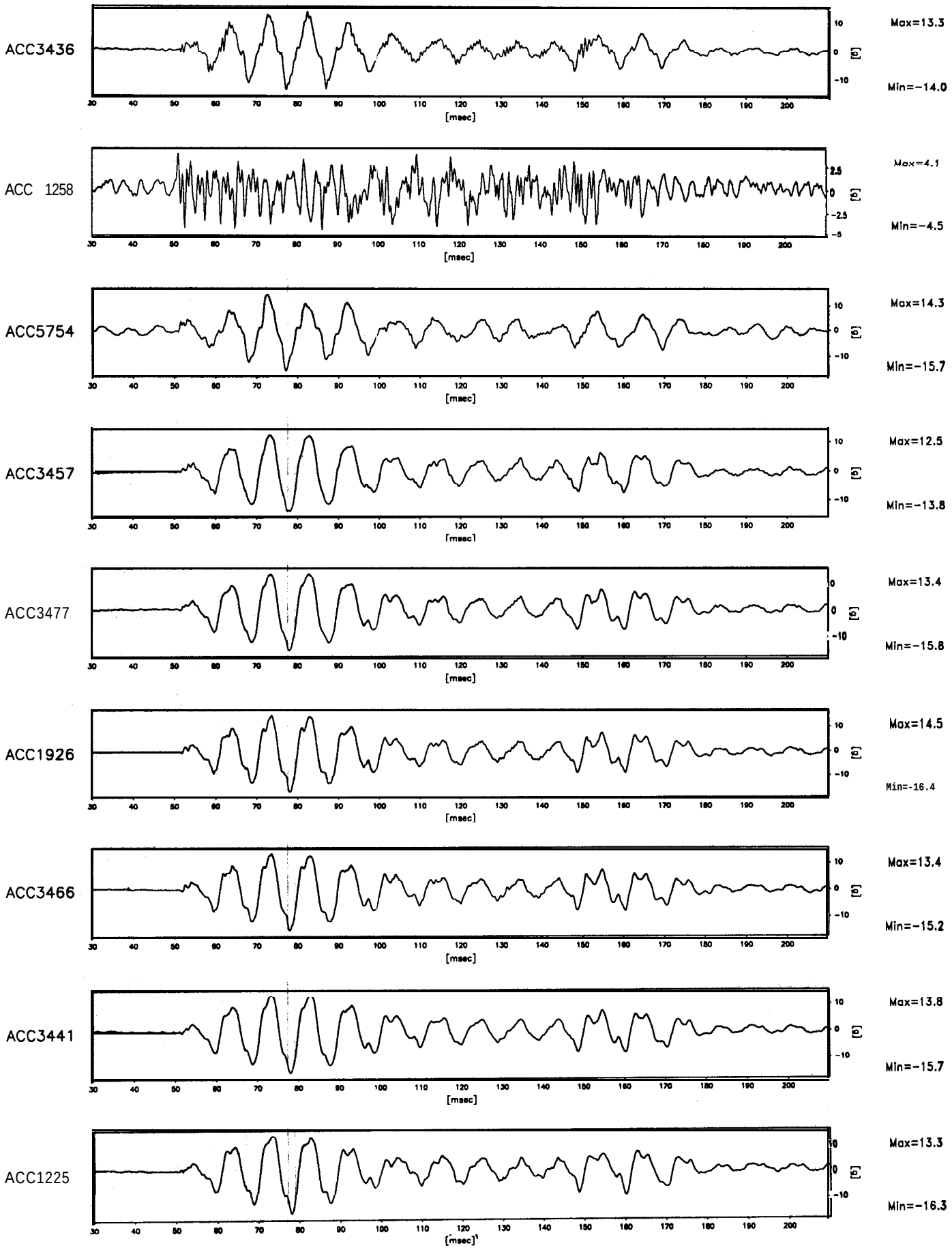

Scales : Model

TEST MG-1 MODEL DRY FLIGHT -1	EQ-5	SHORT TERM TIME RECORDS	G Level 60	FIG.NO. **26**

601 data points plotted per complete transducer record

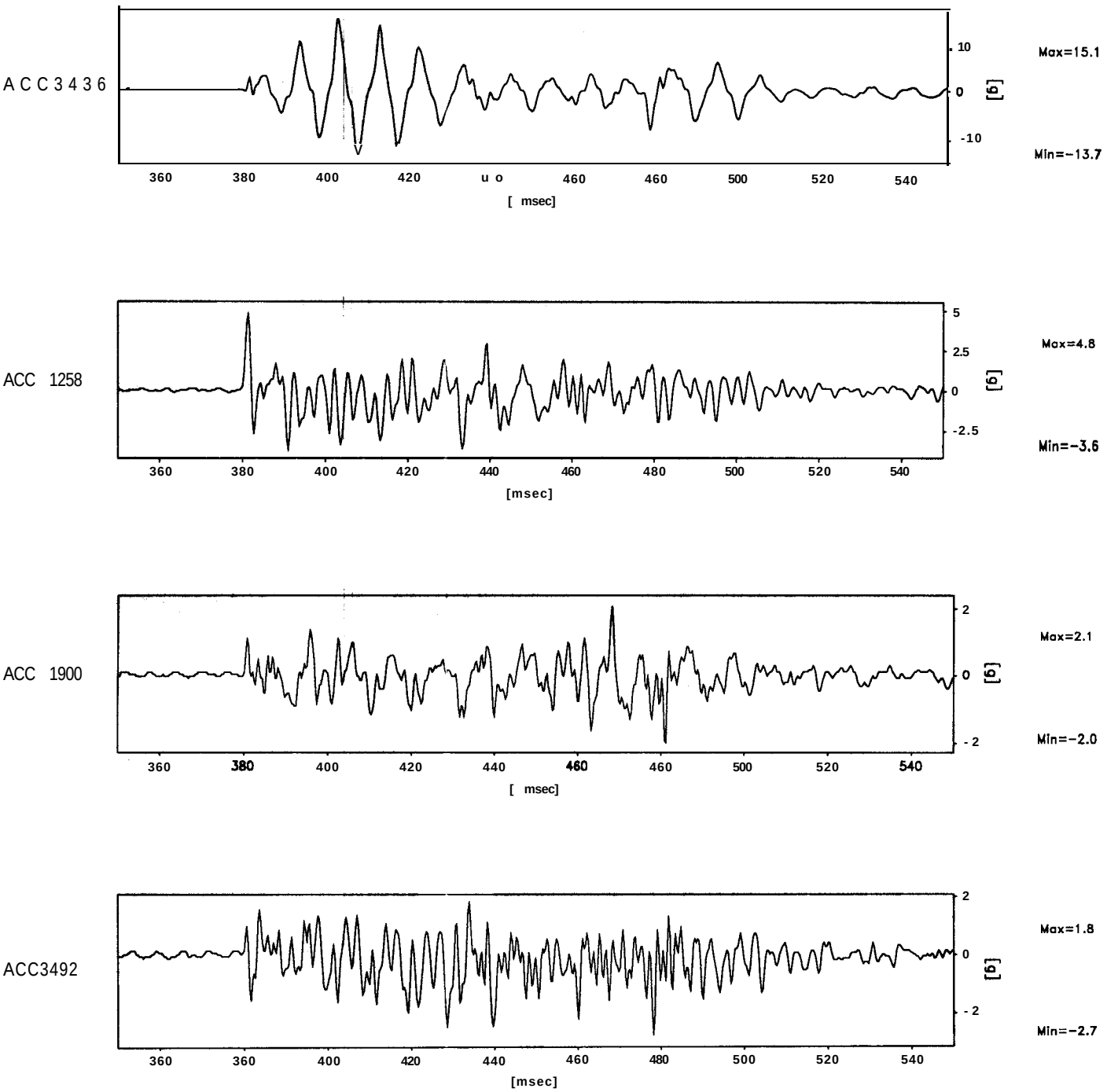

Scales : Model

TEST MG-1 MODEL DRY FLIGHT -1	EQ-5	SHORT TERM TIME RECORDS	G Level 60	FIG.NO. 27

1152 data points plotted per complete transducer record

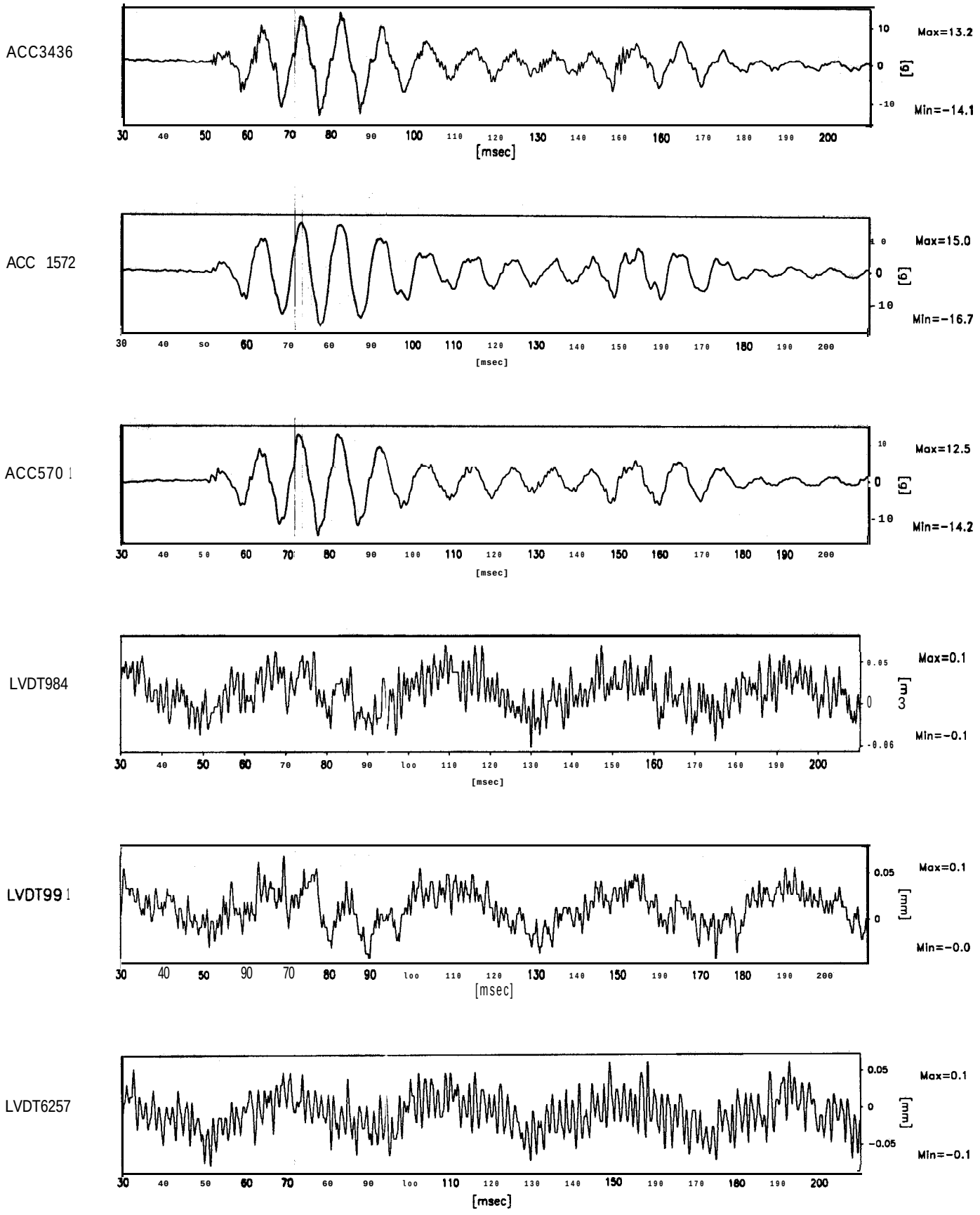

Scales : Model

TEST MG-1 MODEL DRY FLIGHT – 1	EQ–5	SHORT TERM TIME RECORDS	G Level 60	FIG.NO. **28**

8.0 Analysis of the data from the centrifuge tests

As explained earlier each of the earthquakes were fired on the empty ESB box at a different 'g' levels so that the dynamic performance of the ESB box can be measured. The ESB box was extensively instrumented using miniature accelerometers and LVDT's as explained earlier. In this section the frequency analyses of the traces recorded during these centrifuge tests will be presented. From these analyses the performance of the ESB box will be determined. In Table 1 the list of earthquakes and the 'g' level at which they were fired was presented. The analyses of the data will be presented in the same order.

8.1 Earthquake 1 fired at 40 g

The data from this earthquake are presented in Figs.14 to 16. The maximum acceleration recorded by the base accelerometer 3436 during this earthquake was 14.8 %. The strength of the vertical acceleration was 12.2 % which is relatively large when compared with the horizontal acceleration. The base shaking is predominantly at a single frequency with most of the energy of the earthquake concentrated at 87.5 Hz. This uniform base shaking is recorded by all of the accelerometers located at the base of the ESB box, for example as indicated by the traces recorded by ACC's 3436, 5'154, 1572 and 5701 in Figs.14 and 16. The location of these transducers is given in Fig.12. However there is a second higher frequency component in the traces recorded by accelerometers placed at a distance above the base of the ESB box. For example consider the traces in Fig.14 recorded by ACC's 3457, 3477 and 1926 on the right hand side end wall of the ESB box and ACC's 3466, 3441 and 1225 on the left hand side end wall of the ESB box (see Fig.12 for location of these transducers). By comparing the traces of ACC's 3457, 3477 and 1926 in the above figure it can be seen that the strength of the high frequency component increases with the increase of the height at which the accelerometer is placed. The frequency analyses of the base accelerometer 3436 and one of the accelerometers at the top of the end wall ACC 1225 together with the time traces are presented in Fig.29. It can be seen from this figure that the response of the ESB box at 265.0 Hz is significantly amplified. It may be concluded from these observations that the ESB box has a resonant frequency of 265 Hz when subjected to model earthquakes at 40 g.

In Fig.30 the vertical acceleration recorded at the base of the ESB box by ACC 1258 and at the top of both the end walls by ACC 1900 and 3492 are presented (see Fig.12 for the location of the transducers). The corresponding frequency analyses of each of these traces is presented on the right hand side of this figure. The main vertical frequency of the model earthquake at this 'g' level is at 252.0 Hz. This frequency is reflected in the traces recorded at the top of the end walls. The high frequency components are significantly amplified as indicated by the frequency analysis of ACC's 1900 and 3492. Also the frequency content of these accelerometers on either of the end walls does not match suggesting the rocking of the ESB box.

The LVDT's did not record any significant movement of the end walls during this earthquake.

data paints platted per complete transducer record

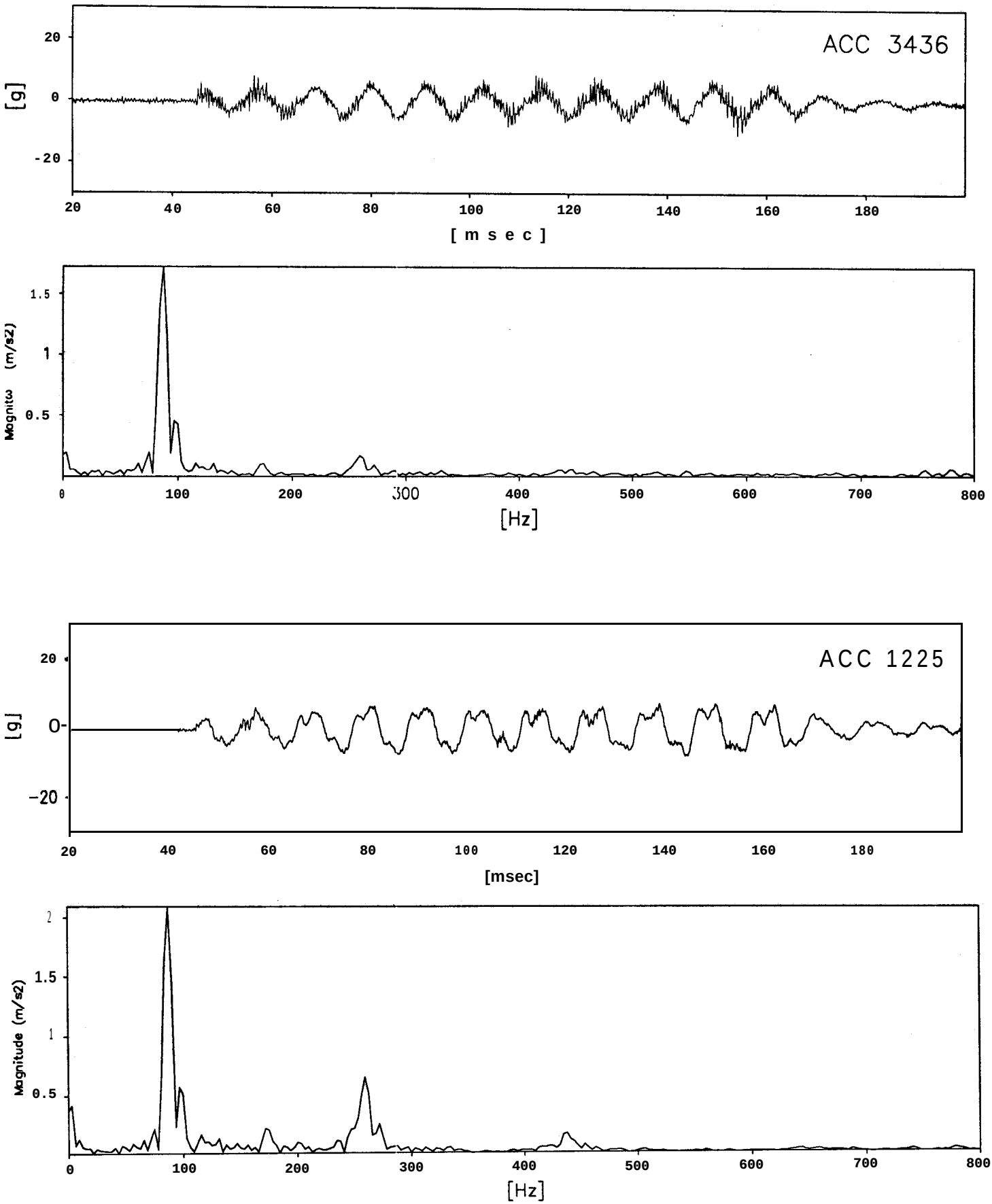

Scales : Model

TEST MODEL FLIGHT	MG-1 EQ-1	TIME RECORDS		FIG.NO. 29

data paints plotted per complete transducer record

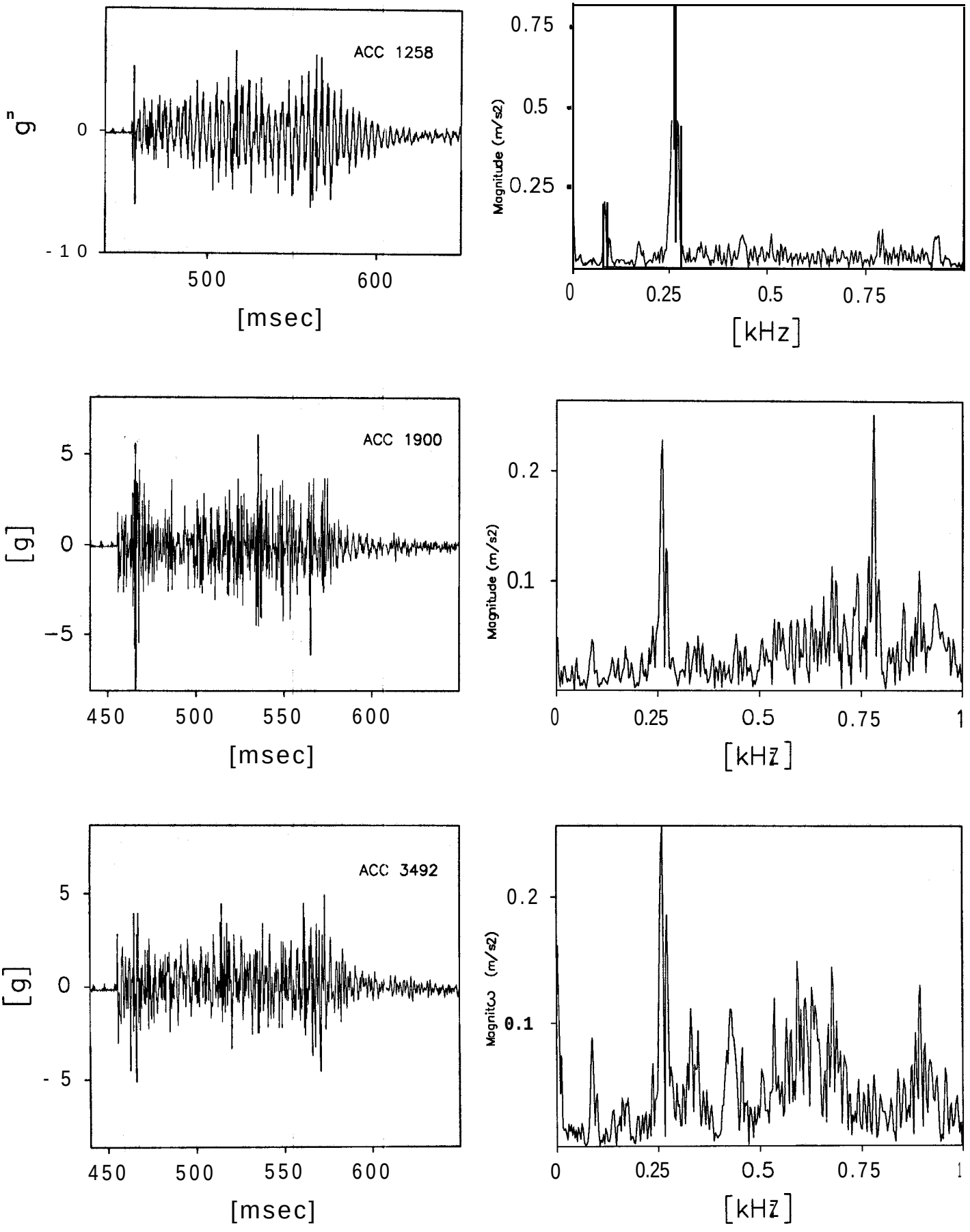

Scales : Model

TEST MODEL FLIGHT	MG-1 EQ-1	TIME RECORDS		FIG.NO. 30

8.2 Earthquake 2 fired at 50 g

The data from this earthquake are presented in Figs.17 to 19. The maximum acceleration recorded by the base accelerometer 3436 during this earthquake was 25.5 %. The peak strength of the vertical acceleration was 19.4 % which is relatively large when compared with the horizontal acceleration. The base shaking is predominantly at a single frequency with most of the energy of the earthquake concentrated at 96.9 Hz. This uniform base shaking is recorded by all of the accelerometers located at the base of the ESB box, for example as indicated by the traces recorded by ACC's 3436, 5'154, 1572 and 5701 in Figs.17 and 19. The location of these transducers is given in Fig.12. There is a second higher frequency component in the traces recorded by accelerometers placed at a distance above the base of the ESB box. For example consider the traces in Figs.17 recorded by ACC's 3457, 3477 and 1926 on the right hand side end wall of the ESB box and ACC's 3466, 3441 and 1225 on the left hand side end wall of the ESB box (see Fig.12 for location of these transducers). By comparing the traces of ACC's 3457, 3477 and 1926 in the above: figure it can be seen that the strength of the high frequency component increases with the increase of the height at which the accelerometer is placed. However, the magnitude of this higher frequency component is much smaller than the one recorded in the 40 g earthquake. The frequency analyses of the base accelerometer 3436 and one of the accelerometers at the top of the end wall ACC 1225 together with the time traces are presented in Fig.31. It can be seen from this figure that the response of the ESB box at 294.0 Hz has no significant amplification.

In Fig.32 the vertical acceleration recorded at the base of the ESB box by ACC 1258 and at the top of both the end walls by ACC 1900 and 3492 are presented (see Fig.12 for the location of the transducers). The corresponding frequency analyses of each of these traces is presented on the right hand side of this figure. The main vertical frequency of the model earthquake at this 'g' level is at 279.0 Hz. This frequency is reflected in the traces recorded at the top of the end walls. The high frequency components are significantly amplified as indicated by the frequency analysis of ACC's 1900 and 3492. Also the frequency content of these accelerometers on either of the end walls is similar suggesting there is very little rocking of the ESB box.

The LVDT's did not record any significant movement of the end walls during this earthquake.

data points plotted per complete transducer record

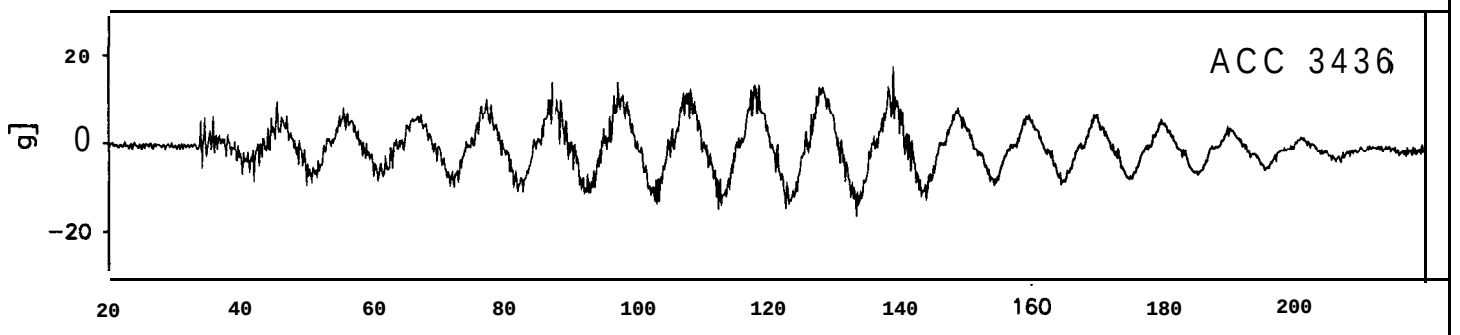

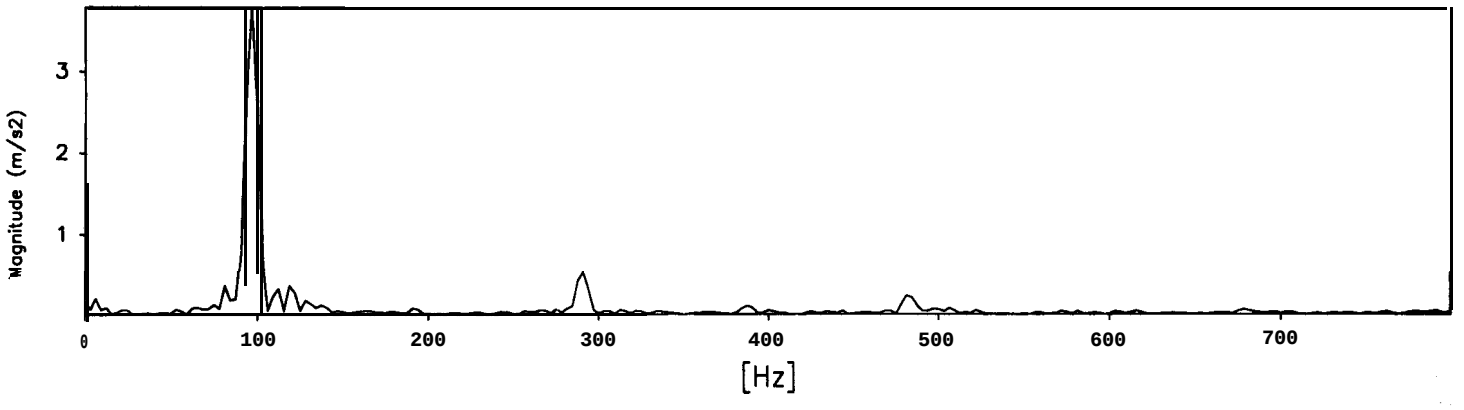

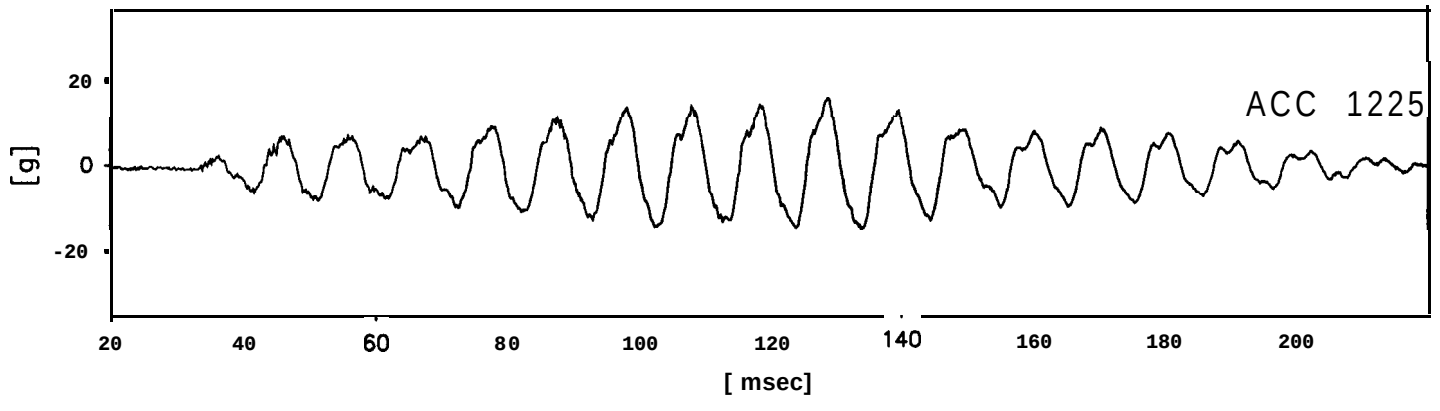

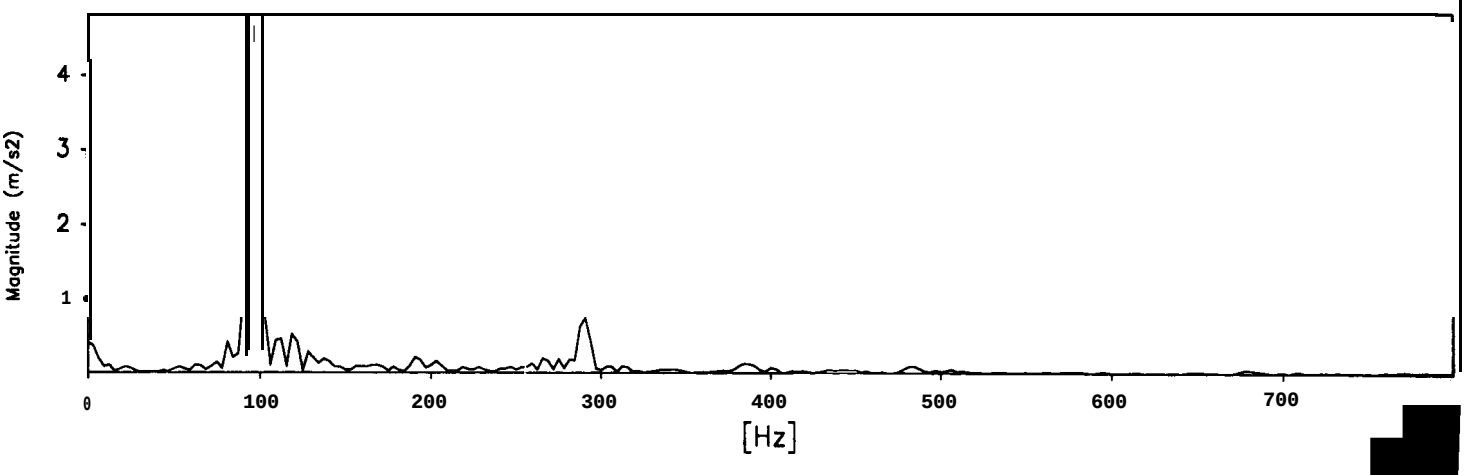

Scales : Model

TEST MODEL FLIGHT	MG-1 EQ-2	TIME RECORDS		FIG.NO. 31

data paints plotted per complete transducer record

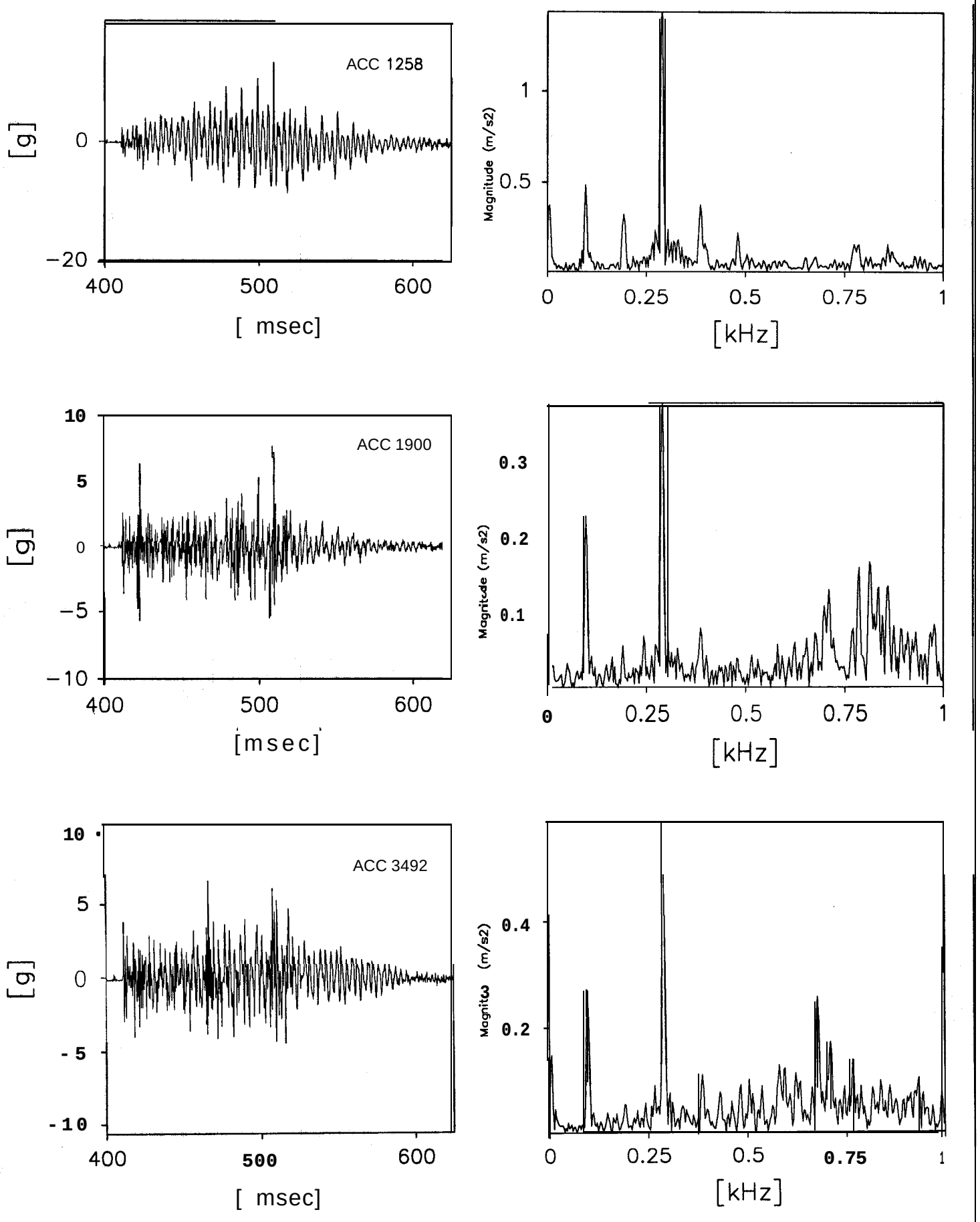

Scales : Model

TEST MODEL FLIGHT	MG-1 EQ-2	TIME RECORDS		FIG.NO. 32

8.3 Earthquake 3jired at 70 g

The data from this earthquake are presented in Figs.20 to 22. The maximum acceleration recorded by the base accelerometer 3436 during this earthquake was 19.3 %. The peak strength of the vertical acceleration was 8.8 %. This is relatively small compared to the horizontal acceleration. The base shaking is predominantly at a single frequency with most of the energy of the earthquake concentrated at 115.7 Hz. This uniform base shaking is recorded by all of the accelerometers located at the base of the ESB box, for example as indicated by the traces recorded by ACC's 3436, 5754, 1572 and 5701 in Figs.20 and 22. The location of these transducers is given in Fig.12. There is a second higher frequency component in the traces recorded by accelerometers placed at a distance above the base of the ESB box. For example consider the traces in Fig.20 recorded by ACC's 3457, 3477 and 1926 on the right hand side end wall of the ESB box and ACC's 3466, 3441 and 1225 on the left hand side end wall of the ESB box (see Fig.12 for location of these transducers). By comparing the traces of ACC's 3457, 3477 and 1926 in the above figure it can be seen that the strength of the high frequency component increases with the increase of the height at which the accelerometer is placed. However, the magnitude of this higher frequency component is much smaller than the one recorded in the 40 g earthquake. The frequency analyses of the base accelerometer 3436 and one of the accelerometers at the top of the end wall ACC 1225 together with the time traces are presented in Fig.33. It can be seen from this figure that the response of the ESB box at 350.0 Hz has no significant amplification.

In Fig.34 the vertical acceleration recorded at the base of the ESB box by ACC 1258 and at the top of both the end walls by ACC 1900 and 3492 are presented (see Fig.12 for the location of the transducers). The corresponding frequency analyses of each of these traces is presented on the right hand side of this figure. The main vertical frequency of the model earthquake at this 'g' level is at 333.2 Hz. This frequency is reflected in the traces recorded at the top of the end walls. However the large component of vertical acceleration recorded by ACC 1258 at 240 Hz is not reflected in the traces recorded by ACC's 1900 and 3492. The high frequency components are significantly amplified as indicated by the frequency analysis of ACC's 1900

and 3492. Also the frequency content of these accelerometers on either of the end walls does not match suggesting there is rocking of the ESB box.

The LVDT's 984 and 991 have recorded a small movement during the earthquake. However the lowest LVDT 6257 did not move during this earthquake confirming that the lowest Dural ring of the ESB box has no relative movement with respect to the base.

data points plotted per complete transducer record

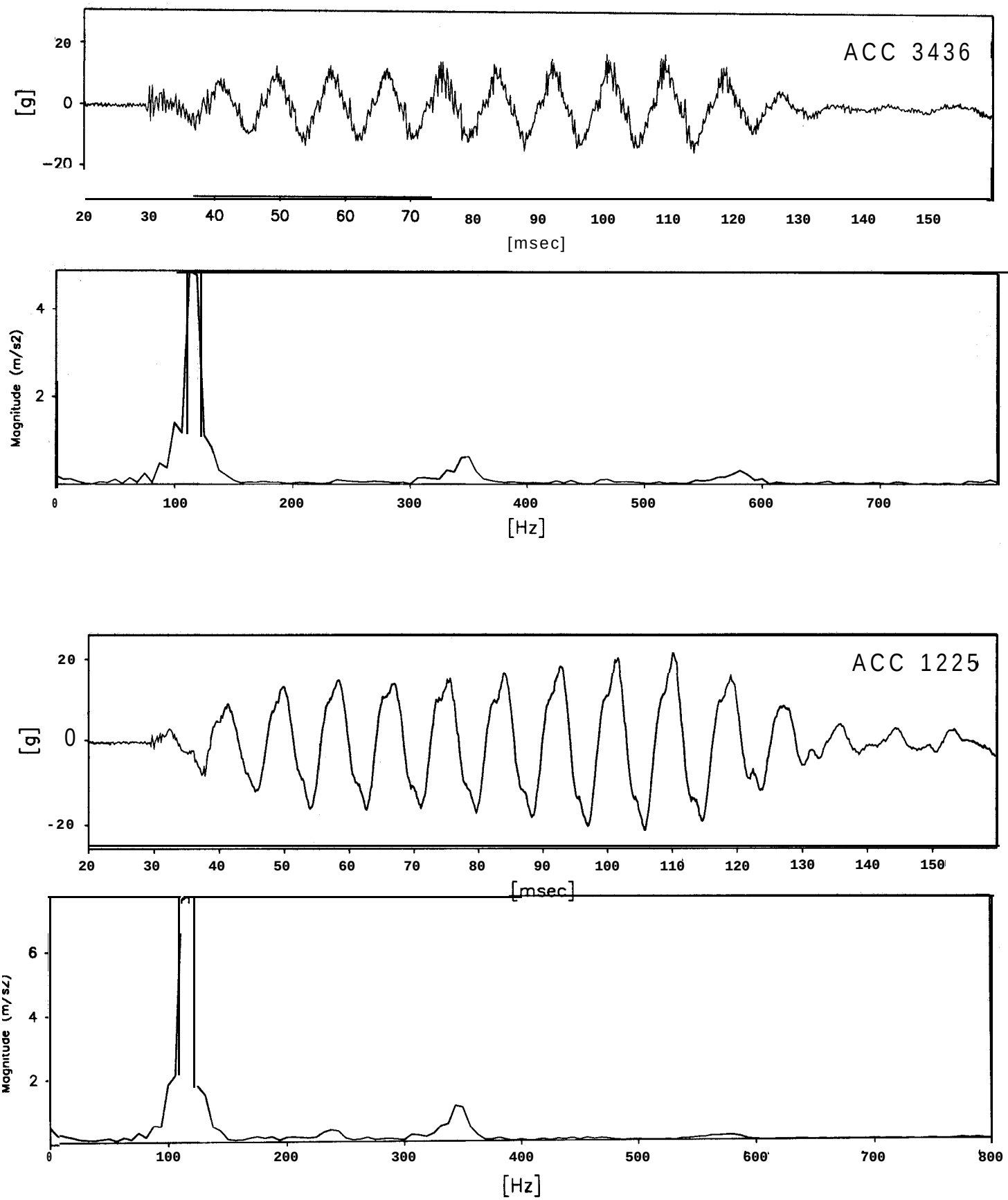

Scales : Model

TEST MODEL FLIGHT	MG-1 E Q - 3	TIME RECORDS		FIG.NO. 33

data points plotted per complete transducer record

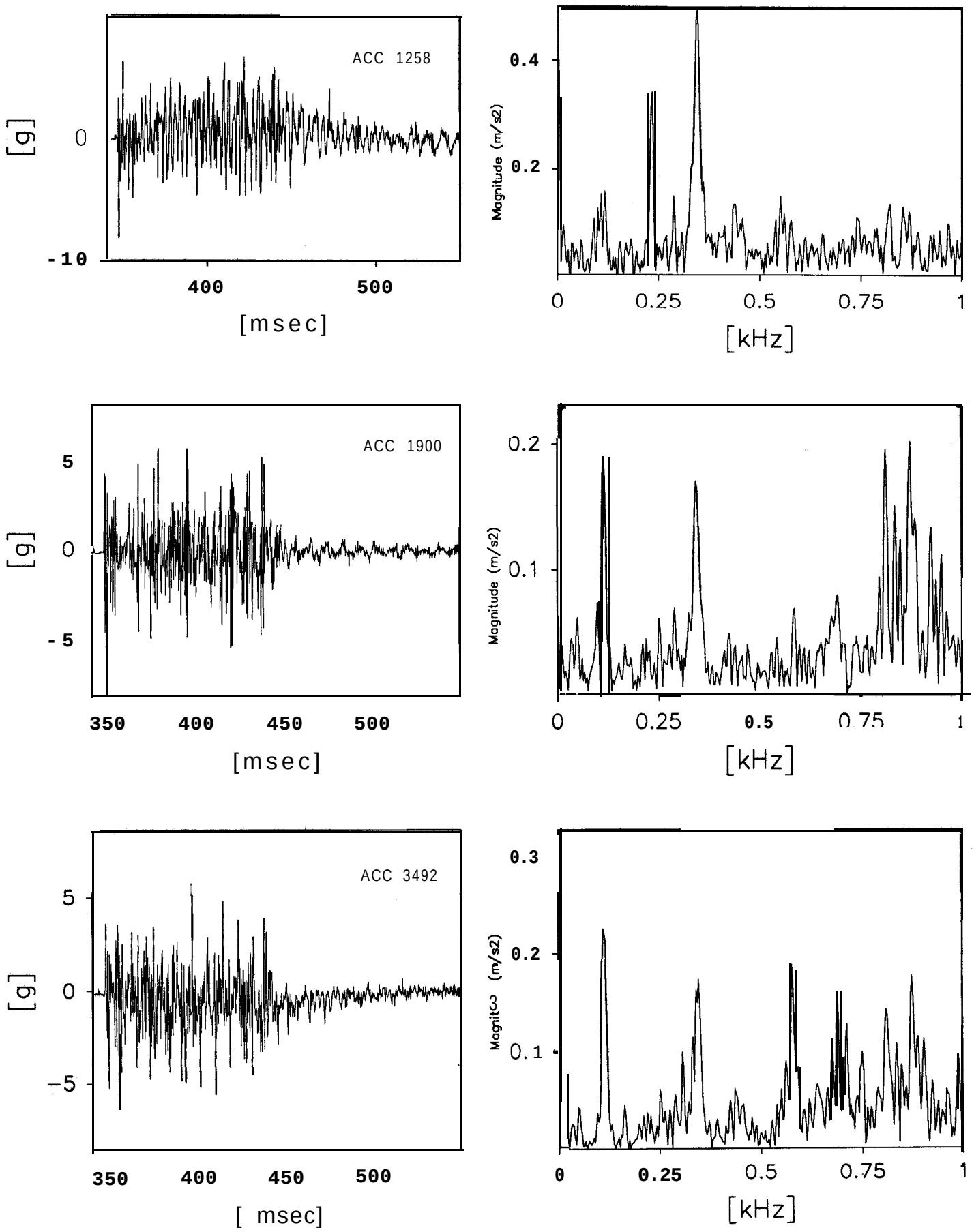

Scales : Model

TEST MODEL FLIGHT	MG-1 EQ-3	TIME RECORDS		FIG.NO. 34

8.4 Earthquake 4 fired at 80 g

Many centrifuge tests in past were conducted at 80 g using the ESB box, Zeng (1991), Madabhushi (1992), etc.,. The data from the earthquake fired at 80 g on the ESB box are presented in Figs.23 to 25. The maximum acceleration recorded by the base accelerometer 3436 during this earthquake was 25.5 %. The peak strength of the vertical acceleration was 9.8 %. This is relatively small compared to the horizontal acceleration. The base shaking is predominantly at a single frequency with most of the energy of the earthquake concentrated at 121.9 Hz. This uniform base shaking is recorded by all of the accelerometers located at the base of the ESB box, for example as indicated by the traces recorded by ACC's 3436, 5754, 1572 and 5701 in Figs.23 and 25. The location of these transducers is given in Fig.12. There is a second higher frequency component in the traces recorded by accelerometers placed at a distance above the base of the ESB box. For example consider the traces in Figs.23 as recorded by ACC's 3457, 3477 and 1926 on the right hand side end wall of the ESB box and ACC's 3466, 3441 and 1225 on the left hand side end wall of the ESB box (see Fig.12 for location of these transducers). By comparing the traces of ACC's 3457, 3477 and 1926 in the above figure it can be seen that the strength of the high frequency component increases with the increase of the height at which the accelerometer is placed. However, the magnitude of this higher frequency component is much smaller than the one recorded in the 40 g earthquake. The frequency analyses of the base accelerometer 3436 and one of the accelerometers at the top of the end wall ACC 1225 together with the time traces are presented in Fig.35. It can be seen from this figure that the response of the ESB box at 377.0 Hz has no significant amplification.

In Fig.36 the vertical acceleration recorded at the base of the ESB box by ACC 1258 and at the top of both the end walls by ACC 1900 and 3492 are presented (see Fig.12 for the location of the transducers). The corresponding frequency analyses of each of these traces is presented on the right hand side of this figure. The main vertical frequency of the model earthquake at this 'g' level is at 35 1.1 Hz. This frequency is reflected in the traces recorded at the top of the end walls. There is a DC drag in the traces recorded by ACC's 1258 and 3492. This may be due to a drag on the amplifier bank and may not indicate a real event. However this downward drag

introduces a large component at rhe zero frequency mark in the frequency analyses of these accelerometers. The high frequency components are significantly amplified as indicated by the frequency analysis of ACC's 1900 and 3492. Also the frequency content of these accelerometers on either of the end walls does not match suggesting there is rocking of the ESB box.

The LVDT's 984 and 991 have recorded a movement of about 0.1 mm during this earthquake. However the lowest LVDT 6257 did not move during this earthquake confirming that the lowest Dural ring of the ESB box has no relative movement with respect to the base. The displacement traces recorded by LVDT's 984 and 991 are in phase suggesting that the end walls are vibrating in their fundamental mode.

data points plotted per complete transducer record

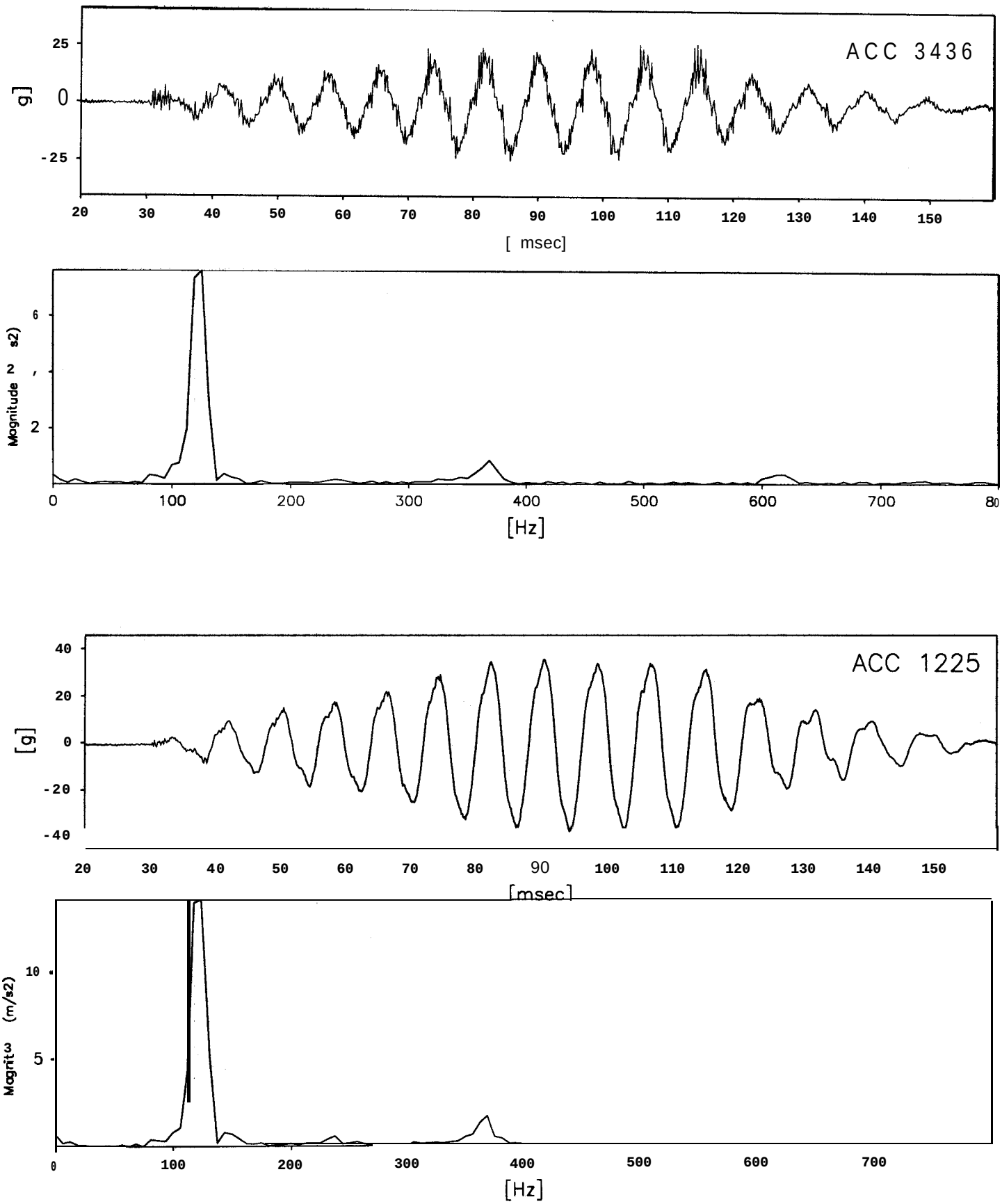

Scales : Model

TEST MODEL FLIGHT	MG-1 EQ-4	TIME RECORDS		FIG.NO. 35

data paints plotted per complete transducer record

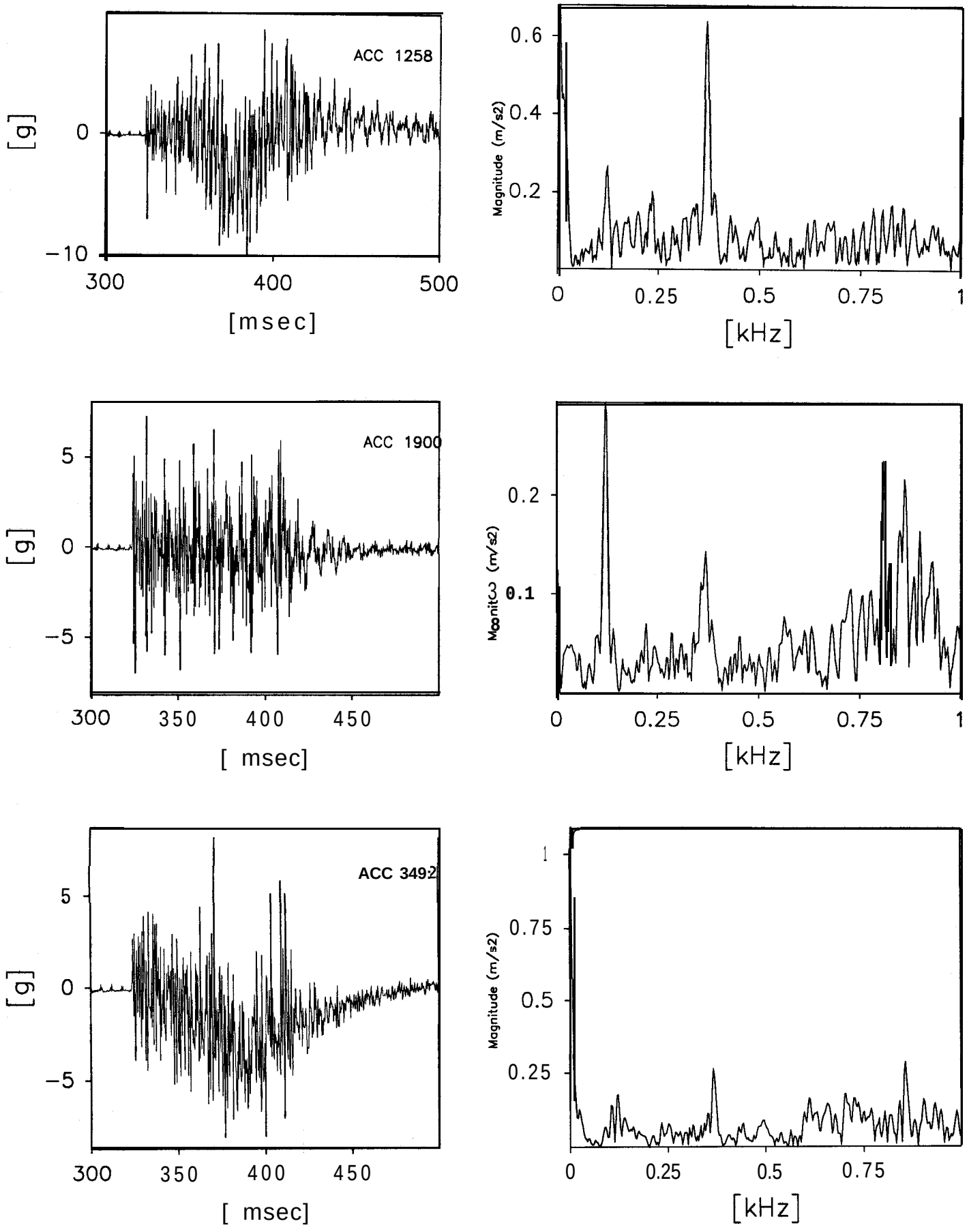

Scales : Model

TEST MODEL FLIGHT	MG-1 **EQ-4**	TIME RECORDS		FIG.NO. 36

8.5 Earthquake 5 fired at 60 g

The bumpy road actuator produces a non uniform earthquake at *60* g. The earthquake is characterised by small amplitude cycles preceded and followed by normal cycles. This feature of the bumpy road is discussed in detail by Madabhushi (1991). The data from the earthquake fired at 60 g on the ESB box are presented in Figs.26 to 28. The maximum acceleration recorded by the base accelerometer 3436 during this earthquake was 14.0 %. The peak strength of the vertical acceleration was 4.5 %. This is relatively small compared to the horizontal acceleration. The base shaking is predominantly at a single frequency with most of the energy of the earthquake concentrated at 100.0 Hz. The base shaking at this frequency and the small amplitude cycles in the middle of the earthquake are recorded by all of the accelerometers located at the base of the ESB box, for example as indicated by the traces recorded by ACC's 3436, 5754, 1572 and 5701 in Figs.26 and 28. The location of these transducers is given in Fig. 12. There is a second higher frequency component in the traces recorded by accelerometers placed at a distance above the base of the ESB box. For example consider the traces in Fig.26 recorded by ACC's 3457, 3477 and 1926 on the right hand side end wall of the ESB box and ACC's 3466, 3441 and 1225 on the left hand side end wall of the ESB box (see Fig. 12 for location of these transducers). By comparing the traces of ACC's 3457, 3477 and 1926 in the above figure it can be seen that the strength of the high frequency component increases with the increase of the height at which the accelerometer is placed. However, the magnitude of this higher frequency component is much smaller than the one recorded in the 40 g earthquake. The frequency analyses of the base accelerometer 3436 and one of the accelerometers at the top of the end wall ACC 1225 together with the time traces are presented in Fig.37. It can be seen from this figure that the response of the ESB box at 3 10.0 Hz has no significant amplification.

In Fig.38 the vertical acceleration recorded at the base of the ESB box by ACC 1258 and at the top of both the end walls by ACC 1900 and 3492 are presented (see Fig.12 for the location of the transducers). The corresponding frequency analyses of each of these traces is presented on the right hand side of this figure. There is no clear main vertical frequency of the model earthquake at this 'g' level apart from the one at driving frequency of the earthquake. The high

frequency components are significantly amplified as indicated by the frequency analysis of ACC's 1900 and 3492. Also the frequency content of these accelerometers on either of the end walls does not match suggesting there is rocking of the ESB box.

The LVDT's did not record any significant movement of the end walls during this earthquake.

9.0 Amplification of the input motion

The horizontal accelerations at the top of the end walls recorded during each of the earthquakes had some amplification compared to the input acceleration. The amplification factor for each earthquake is calculated as a ratio of the peak horizontal acceleration recorded at the top of the end wall to the peak input horizontal acceleration. The accelerometers 1926 and 5754 placed at the top and bottom of the end wall on the right hand side of the ESB box (see Fig.12) were used in the above computation. In 'Table 2 these amplification factors are presented.

Table 2 Amplification Factors for Horizontal Acceleration

Earthquake	G Level	Amplification Factor
EQ-1	40 g	1.1429
EQ-2	50 g	1.1541
EQ-3	70 g	1.2851
EQ-4	80 g	1.3210
EQ-5	60 g	1.0446

The amplification factors increase with the increase of 'g' level with the maximum amplification occurring at 80 g.

A similar calculation is done for the vertical accelerations. In the case of vertical accelerations there is an attenuation of the peak input vertical acceleration though the smaller high frequency components are amplified. The attenuation factor is calculated as the ratio of peak vertical

data points plotted per complete transducer record

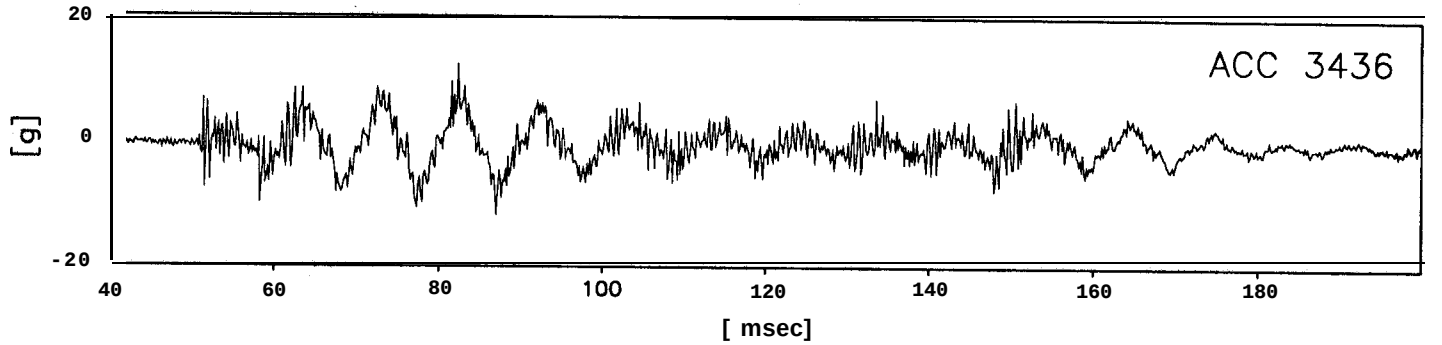

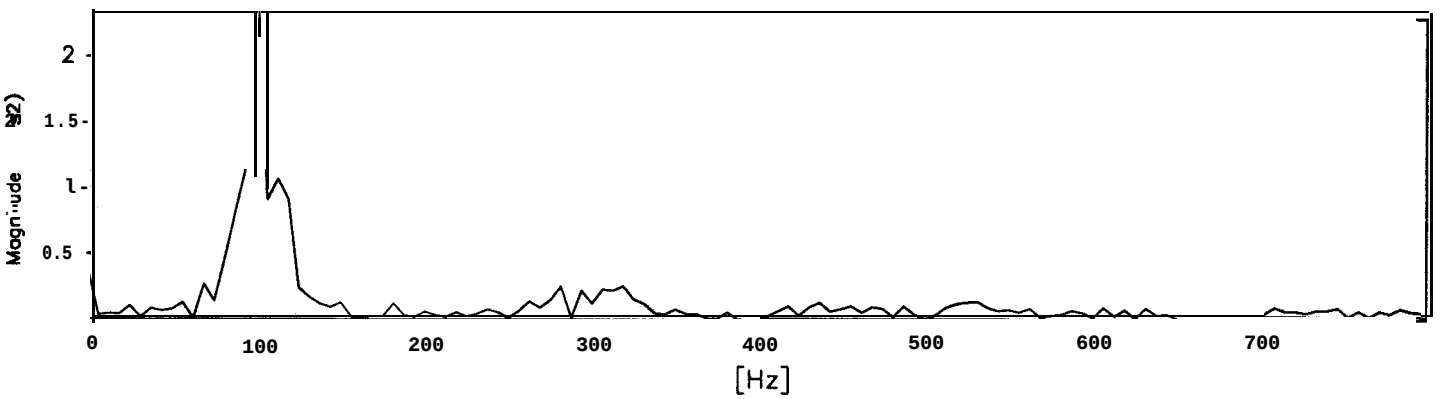

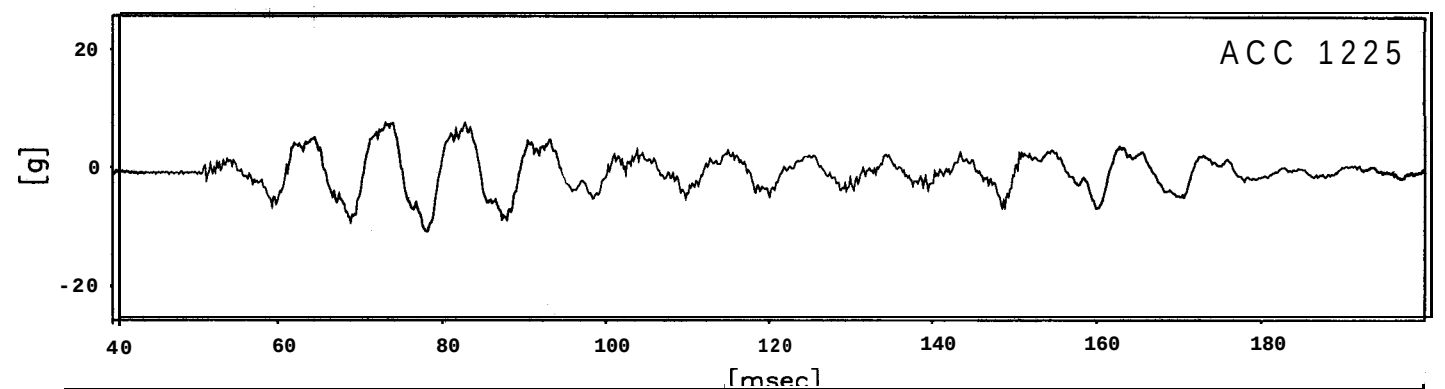

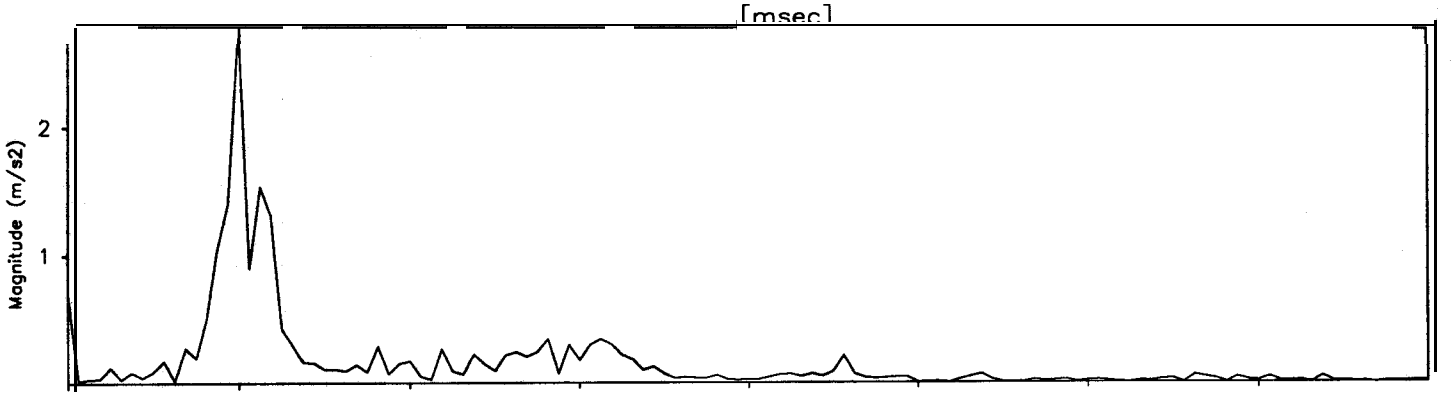

Scales : Model

TEST MODEL FLIGHT	MG-1 EQ-5	TIME RECORDS		FIG.NO. 37

data points plotted per complete transducer record

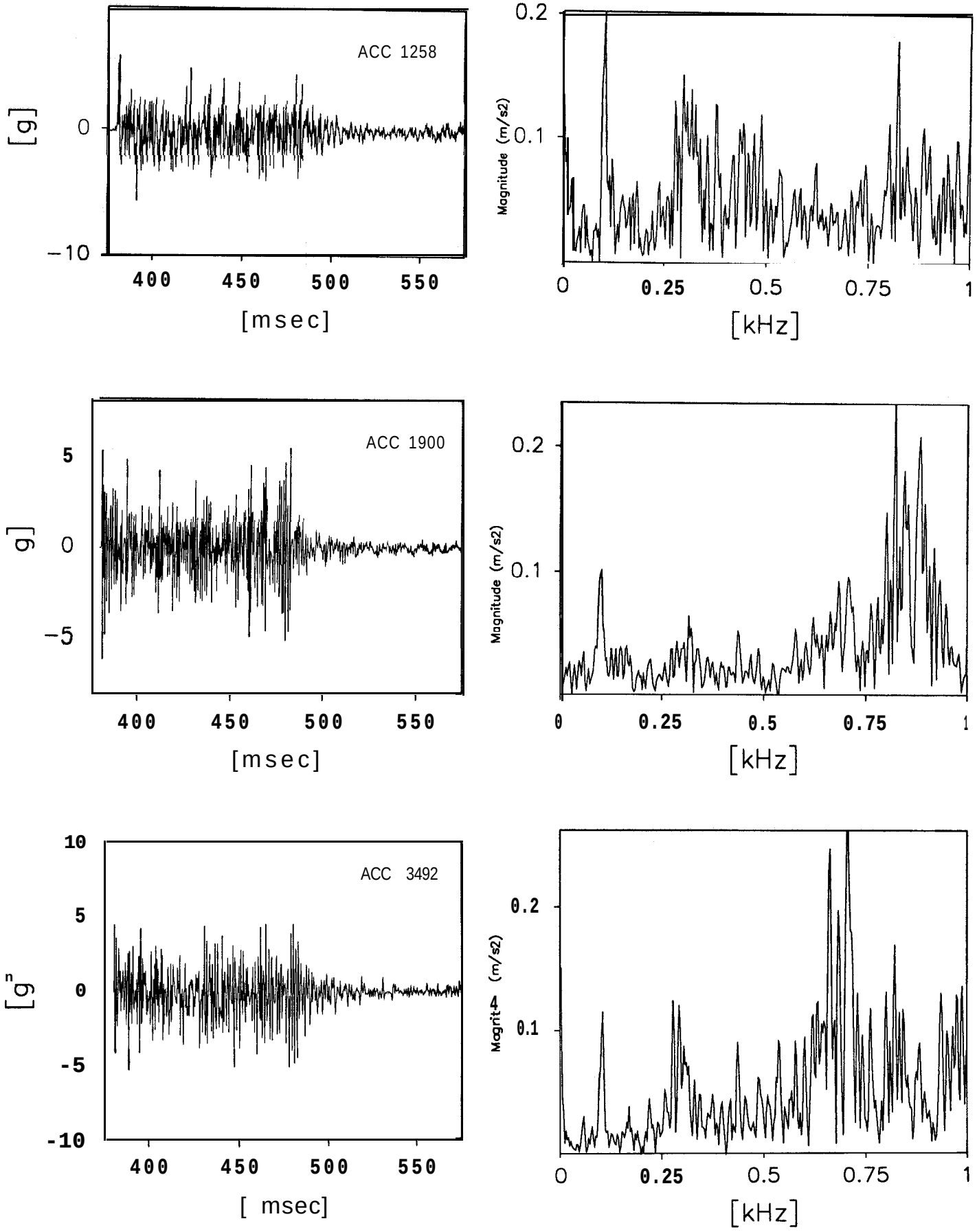

Scales : Model

TEST MODEL FLIGHT	MG-1 EQ-5	TIME RECORDS		FIG.NO. 38

acceleration recorded at the top of the end wall to the peak input vertical acceleration. The accelerometers 3492 and 1258 placed at the top of the end wall and on the base of the ESB box (see Fig.12) were used in the above computation. In Table 3 these attenuation factors are presented.

Table 3 Attenuation Factors for Vertical Acceleration

Earthquake	G Level	Attenuation Factor
EQ-1	40 g	0.5053
EQ-2	50 g	0.4962
EQ-3	70 g	0.8421
EQ-4	80 g	0.8025
EQ-5	60 g	0.75

The vertical accelerations are attenuated the most in the 40g and 50g earthquakes. The attenuation decreases at 70g and 80g. It is interesting to note that the attenuation at 80g is greater than at 70g.

10.0 Conclusions

It is important to simulate the semi-infinite extent of soil in a dynamic centrifuge model test. An Equivalent Shear Beam box was designed and manufactured at the Cambridge University with flexible end walls which simulate the shear deformation of a horizontal soil layer subjected to a model earthquake. The ESB box was designed to match the shear deformation of a 200 mm soil layer subjected to a 30% earthquake at a centrifugal acceleration of 50g. However all these design conditions may not be satisfied in a particular centrifuge test. The performance of the ESB box at different 'g' levels must be known so that it can be used in any practical centrifuge test series.

The dynamic response of this ESB box at different 'g' levels is investigated by conducting a centrifuge test. Several earthquakes were fired on the empty ESB box at different 'g' levels. The data from this test are presented in this report. A detailed analysis of the data suggests that the ESB box amplifies a higher frequency component during an earthquake fired at 40g. This higher frequency component increases in strength along the height of the end wall. However the magnitude of this higher frequency component is small when earthquakes are fired at other 'g' levels namely 50g, 60g, 70g and 80g. The higher frequencies of vertical accelerations are amplified at all the 'g' levels at which earthquakes were fired. The amplification of the peak horizontal acceleration increased with the increase of 'g' level. The peak vertical accelerations however were attenuated even though the higher frequency components of the vertical accelerations were amplified.

REFERENCES

Hardin, B.O. and Drnevich, V.P., (1972), Shear modulus and damping in soils: design equations and curves, Jnl. of Soil Mech. and Found. Eng.Div., ASCE, No.SM7, pp.667-692.

Madabhushi, S.P.G., (1991). Response of tower structures subjected to earthquake perturbations', Ph.d thesis, Cambridge University, England.

Madabhushi, S.P.G. and Zeng, X., (1993), An analysis of the seismic behaviour of quay walls, Proc. Verification of Liquefaction Analyses by Centrifuge studies, (VELACS), Vol.II., K.Arulanandan and R.F.Scott (Editors), Davis, Caliiornia.

Schofield, A.N. and Zeng, X., (1992), Design and performance of an equivalent-shear-beam (ESB) container for earthquake centrifuge modelling, Technical Report, CUED/D-Soils /TR245, Cambridge University, England.

Steedman, R.S., (1991), Centrifuge modelling for dynamic geotechnical studies, Second Int. Conf. on Rec.Adv. in Geo. and Earthquake Eng. and Soil Dynamics, St.Louis, Missouri, USA.

Zeng, X., (1991), Design of the Cambridge Dynamic Shear Box, Technical Report, CUED/D-Soils/TR241, Cambridge University, England.